Experimental and Theoretical Analysis of the Hydrogen-bonding Motifs Formed Between the Carboxyl and the Carboxylate Group: Towards a Systematic Classification of their Supramolecular Motifs

P. Rodríguez-Cuamatzi[a]; O. I. Arillo-Flores[a]; M. I. Bernal-Uruchurtu[a]; H. Höpfl[a]

[a] Centro de Investigaciones Químicas, Universidad Autónoma del Estado de Morelos, Cuernavaca, México

PLEASE SCROLL DOWN FOR ARTICLE

Experimental and Theoretical Analysis of the Hydrogen-bonding Motifs Formed Between the Carboxyl and the Carboxylate Group: Towards a Systematic Classification of their Supramolecular Motifs

P. RODRÍGUEZ-CUAMATZI, O. I. ARILLO-FLORES, M. I. BERNAL-URUCHURTU and H. HÖPFL*

Centro de Investigaciones Químicas, Universidad Autónoma del Estado de Morelos, Av. Universidad 1001, C.P. 62209 Cuernavaca, México

Nine tetraalkylammonium salts, with R = Me, Et, *n*Pr and *n*Bu, of four different carboxylic acids, namely isophthalic acid, 5-nitroisophthalic acid, trimesic acid and pyromellitic acid (1,2,4,5-benzenetetracarboxylic acid), have been prepared and their supramolecular structures analyzed by X-ray crystallography. The [RCOOH···HOOCR] homodimeric motif characteristic for carboxylic acids has not been detected, but instead, in all compounds a [RCOOH···OOCR]⁻ unit was present. The hydrogen-bonding geometries and interaction energies of the different discrete and water-expanded hydrogen-bonding patterns formed between the carboxyl and the carboxylate group have been analyzed systematically by theoretical calculations at the MP2/6-31G(d,p) level of theory.

Carboxylates are promising candidates for crystal engineering and [O—H···O]⁻ interactions play an important role for the structural organization and chemistry of biomolecules.

INTRODUCTION

Supramolecular chemists and crystal engineers aim at control of the mutual organization of molecules in space, taking into consideration the attractive and repulsive intermolecular interactions that can exist between them. However, the combination of two or more functional groups through noncovalent interactions with a high degree of predictability for the resulting structure is frequently difficult, mainly because noncovalent interactions have a significantly lower directionality than covalent bonds or even none at all. Furthermore, additional functional groups attached to one of the reagents can interfere, having an inhibiting influence or causing a "side reaction" (formation of another motif). Therefore, for the purposes of crystal engineering it is necessary not only to create a library of synthons for the different functional groups available to the chemist, but also to have access to tables of physical parameters such as the interaction energies. An important obstacle for the realization of this purpose is that the strength of noncovalent interactions can vary significantly, e.g., through variations in the supramolecular organization or the presence of solvent molecules that can participate in the intermolecular aggregation process.

Among the functional groups used most frequently for supramolecular synthesis and crystal engineering are carboxyl groups and their derivatives [1–8]. The reason is that these functions are capable of forming robust and directional hydrogen-bonds, thus allowing for a reasonably good control over the resulting structures. Many of the organic, metalorganic and organometallic 2D and 3D supramolecular structures of carboxylic acids are porous or possess cavities, and have therefore received much attention [9–43].

The most prominent hydrogen-bonding motif for carboxylic acids is the homodimer (motif **A**, Chart 1), however, it is also possible that two COOH groups are linked through only one hydrogen bond

*Corresponding author. E-mail: hhopfl@ciq.uaem.mx

A   *syn*-**B**   *anti*-**B**

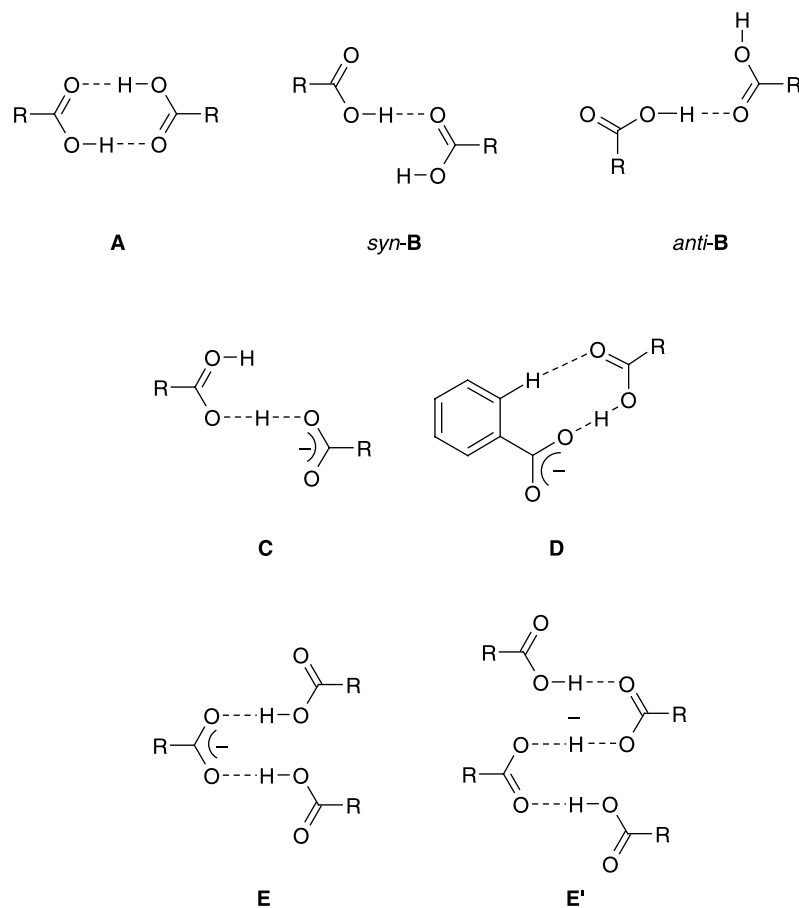**C**   **D**

E   **E'**

CHART 1   Hydrogen-bonding motifs formed between carboxylic acids and carboxylates.

(motif **B**, Chart 1). An almost infinite number of conformations are possible, considering that (i) the hydrogen atoms in the carboxyl groups can have *syn* or *anti* configuration, (ii) the dihedral angle between the carboxyl groups can have values varying from 0 to 360° [44–48].

The intermolecular bond formed between carboxyl groups can be modified in several ways, e.g., through (i) the introduction of additional functional groups in organic moieties attached to the —COOH function, (ii) the deprotonation of part of the carboxyl groups giving rise to motifs **C**, **D** and **E** (Chart 1), and (iii) the introduction of additional molecules with the capacity for hydrogen-bond formation, such as water or alcohols, whose function may be described as "spacer" or "bond strength modulator" (motifs **F**−**M** in Chart 2).

Since charged [RCOOH···OOCR]⁻ systems form significantly stronger hydrogen bonds than the [RCOOH···HOOCR] dimers (≈ − 31 kcal/mol ↔ ≈ − 19 kcal/mol) [49], recently carboxylate based systems have been the subject of several studies in crystal engineering [50–64]. Such systems, and in particular those having [RCOOH···OOCR]⁻ and [ROH···OOCR]⁻ interactions, play also an

important role for the structural organization and chemistry of biomolecules [65–68].

As already mentioned, for supramolecular synthesis and crystal engineering it is convenient to use robust synthons with high interaction energies [67], and therefore, we became interested in a systematic examination of the hydrogen-bonding interactions formed between carboxylates and carboxylic acids. In order to reduce the non-covalent interactions between the anionic targets and the cationic counterpart to a minimum, we used tetraalkyl-ammonium moieties as counterions and examined the salts of the following four carboxylic acids: isophthalic acid (H₂IPA), 5-nitroisophthalic acid (H₂NIPA), trimesic acid (H₃TMA) and pyromellitic acid (1,2,4,5-benzenetetracarboxylic acid, H₄PMA). Their supramolecular structures were examined in the solid state by X-ray crystallographic studies, and once the prominent hydrogen-bonding motifs occurring in the solid state had been characterized, we performed *ab initio* calculations for a comparative structural analysis and to analyze their relative strength. Four different alkyl ammonium salts were employed (R = Me, Et, *n*Pr and *n*Bu) to evaluate also the influence of the counterion volume on the supramolecular structure.
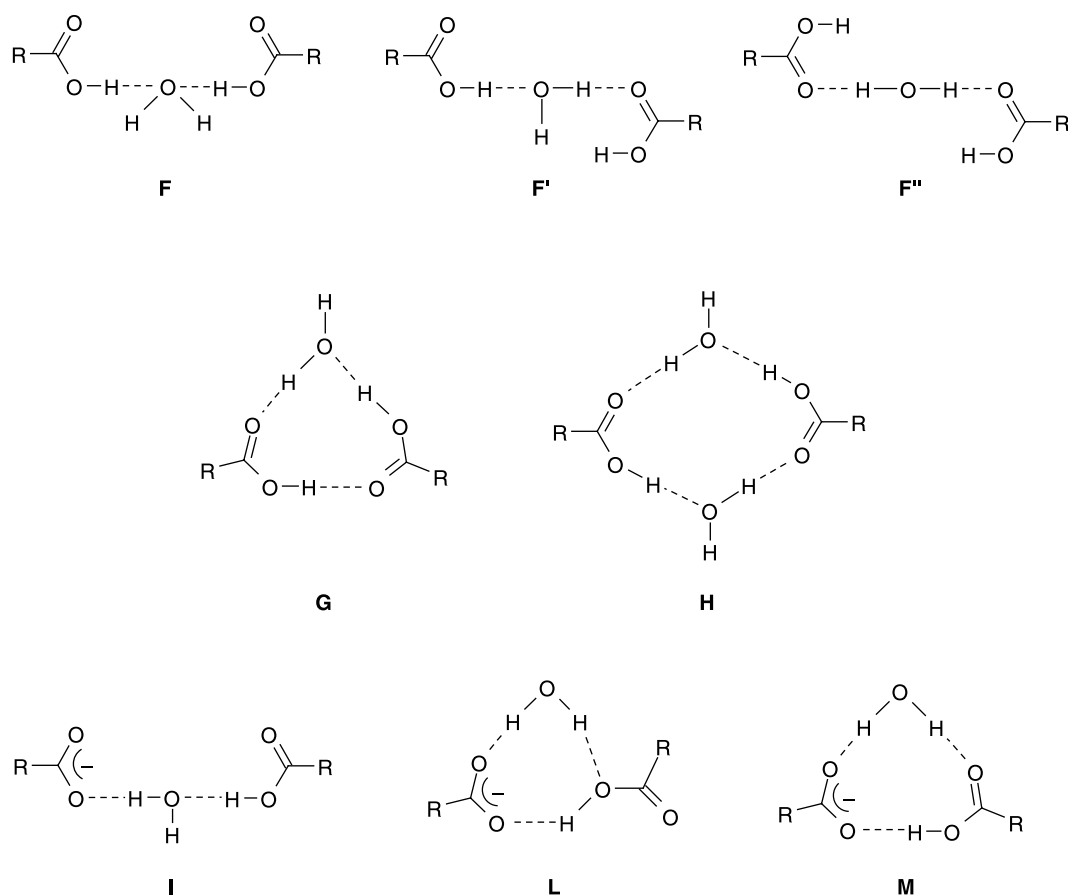
CHART 2 Expanded hydrogen-bonding motifs formed between carboxylic acids and carboxylates in the presence of water molecules.

EXPERIMENTAL SECTION

Preparative Part

Preparation of Crystals from Isophthalic Acid and Tetra-n-butylammonium Hydroxide 1

To a solution of isophthalic acid (0.50 g, 3.00 mmol) in ethanol (8 mL) tetra-*n*-butylammonium hydroxide (0.78 g, 3.00 mmol) was added. The solution was stirred for 15 mins., whereupon the solvent was eliminated under vacuum. Recrystallization from ethanol provided **1** in form of light-yellow crystals that were suitable for X-ray crystallography. Yield: 65%; m.p. 260–264°C.

IR(KBr): $\tilde{v} = 3405$ (m), 3072 (w), 2962 (s), 2875 (m), 1723 (w), 1667 (w), 1611 (w), 1566 (w), 1483 (w), 1383 (m), 1158 (w), 1064 (w), 1030 (w), 887 (w), 741 (m), 677 (w), 505 (w) cm^{-1}.

Preparation of Crystals from 5-Nitroisophthalic Acid and Tetramethylammonium Hydroxide 2

To a solution of 5-nitroisophthalic acid (0.50 g, 2.36 mmol) in ethanol (8 mL) tetramethylammonium hydroxide (0.22 g, 2.36 mmol) was added. The solution

was stirred for 15 mins., whereupon the solvent was eliminated under vacuum. Recrystallization from ethanol provided **2** in form of light-yellow crystals that were suitable for X-ray crystallography. Yield: 75%; m.p. 188–190°C.

IR (KBr): $\tilde{v} = 3372$ (m), 3219 (w), 3117(w), 3065 (w), 1721 (s), 1666 (s) 1543 (s), 1486 (m), 1348 (m), 1329 (m), 1313 (s), 1229 (s), 731 (s), 705 (m), 684 (s), 671 (m), 616 (w), 602 (w) cm^{-1}.

Preparation of Crystals from 5-Nitroisophthalic Acid and Tetraethylammonium Hydroxide 3

To a solution of 5-nitroisophthalic acid (0.50 g, 2.36 mmol) in ethanol (8 mL) tetraethylammonium hydroxide (0.35 g, 2.36 mmol) was added. The solution was stirred for 15 mins., whereupon the solvent was eliminated under vacuum. Recrystallization from ethanol provided **3** in form of light-yellow crystals that were suitable for X-ray crystallography. Yield: 70%; m.p. 232–233°C.

IR (KBr): $\tilde{v} = 3442$ (w), 3111 (w), 3059 (w), 2996 (w), 1730 (s), 1539 (m), 1482 (w), 1353 (m), 1226 (m), 1169 (m), 1078 (w), 1006 (w), 798 (w), 734 (w), 696 (m), 671 (m), 488 (w) cm^{-1}.

Preparation of Crystals from 5-Nitroisophthalic Acid and Tetra-n-propylammonium Hydroxide 4

To a solution of 5-nitroisophthalic acid (0.50 g, 2.36 mmol) in ethanol (8 mL) tetra-*n*-propylammonium hydroxide (0.48 g, 2.36 mmol) was added. The solution was stirred for 15 mins., whereupon the solvent was eliminated under vacuum. Recrystallization from ethanol provided **4** in form of light-yellow crystals that were suitable for X-ray crystallography. Yield: 72%; m.p. 177–182°C.

IR (KBr): $\tilde{\nu} = 3455$ (w), 3099 (w), 2976 (w), 1715 (s), 1627 (w), 1536 (m), 1464 (w), 1348 (m), 1257 (w), 1214 (w), 1176 (w), 1083 (w), 969 (w), 812 (w), 777 (w), 731 (w), 702 (w), 669 (w) cm^{-1}.

Preparation of Crystals from 5-Nitroisophthalic Acid and Tetra-n-butylammonium Hydroxide 5

To a solution of 5-nitroisophthalic acid (0.50 g, 2.36 mmol) in ethanol (8 mL) tetra-*n*-butylammonium hydroxide (0.61 g, 2.36 mmol) was added. The solution was stirred for 15 mins., whereupon the solvent was eliminated under vacuum. Recrystallization from ethanol provided **5** in form of light-yellow crystals that were suitable for X-ray crystallography. Yield: 75%; m.p. 171–176°C.

IR (KBr): $\tilde{\nu} = 3460$ (w), 3177 (w), 3099 (w), 2969 (w), 2549 (w), 1714 (s), 1629 (w), 1534 (m), 1465 (w), 1353 (m), 1292 (w), 1215 (m), 1172 (w), 1096 (w), 925 (w), 812 (w), 732 (w), 700 (w), 664 (w) cm^{-1}.

Preparation of Crystals from Trimesic Acid and Tetramethylammonium Hydroxide 6

To a solution of trimesic acid (0.50 g, 2.37 mmol) in ethanol (10 mL) tetra-*n*-butylammonium hydroxide (0.22 g, 2.37 mmol) was added. The solution was stirred for 15 mins., whereupon the solvent was eliminated under vacuum. Recrystallization from methanol provided **6** in form of colorless crystals that were suitable for X-ray crystallography. Yield: 83%; m.p. 309–311°C.

IR (KBr): $\tilde{\nu} = 3405$ (w), 3222 (w), 3134 (w), 2922 (w), 2663 (w), 2568 (w), 1920 (w), 1709 (s), 1611 (w), 1569 (w), 1489 (w), 1452 (w), 1371 (w), 1273 (s), 1100 (w), 951 (w), 744 (m), 688 (m), 542 (w) cm^{-1}.

Preparation of Crystals from Trimesic Acid and Tetraethylammonium Hydroxide 7

To a solution of trimesic acid (0.50 g, 2.37 mmol) in ethanol (10 mL) tetra-ethylammonium hydroxide (0.35 g, 2.37 mmol) was added. The solution was stirred for 15 mins., whereupon the solvent was eliminated under vacuum. Recrystallization from ethanol provided **7** in form of colorless crystals that

were suitable for X-ray crystallography. Yield: 70%; m.p. >350°C.

IR (KBr): $\tilde{\nu} = 3454$ (w), 3096 (w), 2663 (w), 2556 (w), 1933 (w), 1709 (s), 1606 (w), 1449 (w), 1405 (w), 1281 (s), 1172 (w), 1001 (w), 837 (w), 785 (w), 745 (m), 686 (m) cm^{-1}.

Preparation of Crystals from Trimesic Acid and Tetra-n-butylammonium Hydroxide 8

To a solution of trimesic acid (0.50 g, 2.37 mmol) in ethanol (10 mL) tetra-*n*-butylammonium hydroxide (0.48 g, 2.37 mmol) was added. The solution was stirred for 15 mins., whereupon the solvent was eliminated under vacuum. Recrystallization from methanol provided **8** in form of colorless crystals that were suitable for X-ray crystallography. Yield: 70%; m.p. 298–303°C.

IR (KBr): $\tilde{\nu} = 3093$ (w), 2979 (w), 2888 (w), 2663 (w), 2550 (w), 1717 (s), 1610 (w), 1565 (w), 1455 (m), 1403 (m), 1277 (s), 933 (w), 750 (m), 687 (m), 542 (w), 429 (w) cm^{-1}.

Preparation of Crystals from Pyromellitic Acid and Tetramethylammonium Hydroxide 9

To a solution of trimesic acid (0.50 g, 1.97 mmol) in methanol (3 mL) tetramethylammonium hydroxide (0.18 g, 1.97 mmol) was added. The solution was stirred for 15 mins., whereupon the solvent was eliminated under vacuum. Recrystallization from methanol/hexane provided **9** in form of colorless crystals that were suitable for X-ray crystallography. Yield: 73%; m.p. 248–252°C.

IR (KBr): $\tilde{\nu} = 3414$ (m), 2963 (d), 2366 (w), 1709 (m), 1613 (w), 1506 (w), 1454 (w), 1388 (w), 1273 (m), 751 (w), 694 (w) cm^{-1}.

X-ray Crystallography

X-ray diffraction studies were performed on a Bruker-AXS diffractometer with a CCD area detector ($\lambda_{MoK\alpha} = 0.71073$ Å, monochromator: graphite). Frames were collected at $T = 100$ K for compounds **5** and **9** and at $T = 293$ K for the remaining compounds via ω and ϕ–rotation ($\Delta/\omega = 0.3°$) at 10 s per frame (SMART) [69]. The measured intensities were reduced to F^2 and corrected for absorption with SADABS (SAINT-NT) [70]. Corrections were made for Lorentz and polarization effects. Structure solution, refinement and data output were carried out with the SHELXTL-NT program package [71,72]. Non hydrogen atoms were refined anisotropically. C—H hydrogen atoms were placed in geometrically calculated positions using a riding model (0.95 Å). O—H hydrogen atoms could be localized by difference Fourier maps and have been refined fixing the isotropic temperature factors

to a value 1.5 times that of the corresponding oxygen atom. For O_w-H hydrogen atoms the bond length has been fixed to 0.84 Å, while for COOH hydrogen atoms the coordinates have been freely refined. In compounds **2**, **3** and **7** the NR_4^+ cations are disordered over two positions, and restraints have been used in order to define the corresponding geometries. Figures were created with SHELXTL-NT [69–72] and MERCURY [73]. Hydrogen bonding interactions in the crystal lattices were calculated by PLATON [74] using the WINGX [75] platform.

Crystallographic data for compounds **1–9** have been deposited with the Cambridge Crystallographic Data Centre as supplementary publications no. CCDC-631691-631699. Copies of the data can be obtained free of charge on application to CCDC, 12 Union Road, Cambridge CB2 1EZ, UK (fax: (+44)1223-336-033; E-mail: deposit@ccdc.cam.ac.uk, website: http://www.ccdc.cam.ac.uk).

DISCUSSION AND RESULTS

Preparation of Compounds 1–9

In order to prepare extended supramolecular structures containing hydrogen-bonding motifs formed between carboxyl groups and carboxylate ions, the four carboxylic acids selected for this purpose were brought to reaction with four different tetraalkylammonium hydroxides, NR_4OH with R = Me, Et, nPr and nBu. Interestingly, despite each acid and base were combined in different proportions (1:1 and 1:2), the composition of the resulting crystalline material was always the same for each pair of reagents, indicating that for each specific combination between acid and base there is a strong preference for one particular hydrogen-bonding motif. Depending on the solubility of the carboxylic acids the crystallization processes were carried out in methanol or ethanol. Nine salts suitable for X-ray crystallography were obtained, whose compositions have been summarized in Table I. The most relevant

crystallographic and hydrogen-bonding parameters are shown in Tables II and III and SI–SV, respectively.

In the case of 5-nitroisophthalic acid all four tetraalkylammonium salts crystallized, so that the influence of the counterion volume on the hydrogen-bonding structure could be analyzed in detail. In the case of trimesic acid three salts could be crystallized, and for isophthalic and pyromellitic acid one salt in each case.

Structural Characterization in the Solid State

Tetra-n-butylammonium Hydrogenisophthalate 1

The X-ray crystallographic study of compound **1**, which has been formed from a solution of tetra-*n*-butylammonium hydroxide and isophthalic acid (H_2IPA) in ethanol, shows that it has the composition $[NBu_4][HIPA][H_2O]$. Together with the water molecules the anionic part of this salt is organized in polymeric hydrogen-bonded supramolecular chains with a zig–zag configuration along axis *c* (Fig. 1). The hydrogen-bonding motif consists of the dimeric motif typically formed between a carboxyl and a carboxylate group, $[RCOOH\cdots OOCR]^-$ (1.20 Å, 1.27 Å, 2.463(2) Å 173°), to which additionally a water molecule is bound. The resulting eight-membered cyclic motif is denominated motif **L** in Chart 2. In this motif the water molecules act as twofold hydrogen donors (O_w—H$\cdots$O2: 0.84 Å, 1.99 Å, 2.817(2) Å, 171° and O_w—H$\cdots$O3': 0.84 Å, 2.24 Å, 2.967(2) Å, 146°). A revision of the CSD database [76] showed that this motif has not been observed so far. In the crystal lattice the anionic chains are separated by perpendicular distances of 7.78 Å, between of which the $[NBu_4]^+$ counterions are located. There are three different C—H$\cdots$O interactions between the cations and the oxygen atoms of the central motif (0.97 Å, 2.624–2.172 Å, 3.545–3.663 Å, 153–167°), which are all within the ranges established previously [77–82].

Tetraalkylammonium 5-nitrohydrogenisophthalates 2–5

As already mentioned in the introduction, in the case of 5-nitroisophthalic acid (H_2NIPA) crystals suitable for X-ray crystallography could be obtained for all four tetraalkylammonium hydroxides. Interestingly, the composition of all four compounds is almost identical, $[NR_4][HNIPA][H_2NIPA]$ with R = Me, Et, nPr and nBu. Only in the case of compound **2** there are also water molecules in the crystal lattice. There are two different types of supramolecular organization, one for the salts with the smaller cations (R = Me, Et), and the other one for the salts with the larger cations (R = nPr, nBu), showing that the volume of the tetraalkylammonium ions plays

TABLE I Compositions of the carboxylic acid–carboxylate adducts studied herein

Compound	Composition[†]
1	$[NBu_4][HIPA][H_2O]$
2	$[NMe_4][HNIPA][H_2NIPA]\cdot 0.5[H_2O]$
3	$[NEt_4][HNIPA][H_2NIPA]$
4	$[NPr_4][HNIPA][H_2NIPA]$
5	$[NBu_4][HNIPA][H_2NIPA]$
6	$[NMe_4][H_2TMA][H_2O]$
7	$[NEt_4][H_2TMA][H_3TMA][H_2O]_2$
8	$[NBu_4][H_2TMA][H_2O]$
9	$[NMe_4][H_3PMA]$

[†]H_2IPA = isophthalic acid, H_2NIPA = 5-nitroisophthalic acid, H_3TMA = trimesic acid, H_4PMA = pyromellitic acid.

TABLE II   Crystallographic data for compounds **1–9**

Crystal data	**1**[†]	**2**[†]	**3**[‡]	**4**[†]	**5**[‡]	**6**[†]	**7**[†]	**8**[†]	**9**[‡]
Formula	$C_{24}H_{43}NO_5$	$C_{40}H_{44}N_6O_{25}$	$C_{24}H_{29}N_3O_{12}$	$C_{28}H_{37}N_3O_{12}$	$C_{32}H_{45}N_3O_{12}$	$C_{13}H_{19}NO_7$	$C_{26}H_{35}NO_{14}$	$C_{25}H_{43}NO_7$	$C_{14}H_{17}NO_8$
Crystal size (mm³)	$0.26 \times 0.41 \times 0.60$	$0.12 \times 0.25 \times 0.52$	$0.16 \times 0.21 \times 0.32$	$0.02 \times 0.09 \times 0.43$	$0.16 \times 0.17 \times 0.37$	$0.12 \times 0.13 \times 0.22$	$0.11 \times 0.17 \times 0.37$	$0.09 \times 0.16 \times 0.33$	$0.21 \times 0.22 \times 0.42$
MW (g mol⁻¹)	425.59	1008.82	551.50	607.61	663.71	301.29	585.54	469.60	327.29
Space group	$P2_1/n$	$P2_1/c$	P-1	$P2_1/c$	$P2_1/c$	$P2_1/n$	P-1	$P2_1/n$	Pnma
Cell parameters									
a (Å)	8.4738(16)	8.6241(9)	7.0742(9)	11.4617(8)	11.827(6)	7.1081(9)	7.6534(7)	9.4472(8)	6.5038(10)
b (Å)	17.528(3)	13.2334(14)	8.6197(11)	13.7275(9)	14.143(7)	16.777(2)	9.5868(9)	18.6383(16)	12.4534(19)
c (Å)	17.235(3)	19.879(2)	11.4112(15)	20.0912(14)	20.121(10)	12.6133(15)	10.9892(11)	15.7236(14)	17.913(3)
α (°)	90	90	91.588(2)	90	90	90	67.098(2)	90	90
β (°)	95.857(3)	94.706(2)	104.826(2)	95.2020(10)	98.039(8)	101.968(2)	74.611(2)	97.378(2)	90
γ (°)	90	90	104.426(2)	90	90	90	71.415(2)	90	90
V (Å³)	2546.5(8)	2261.1(4)	648.34(14)	3148.1(4)	3333(3)	1471.5(3)	694.72(11)	2745.7(4)	1450.9(4)
Z	4	2	1	4	4	4	1	4	4
μ (mm⁻¹)	0.076	0.125	0.115	0.101	0.101	0.111	0.110	0.082	0.124
ρ_{calcd} (g cm⁻³)	1.11	1.48	1.41	1.28	1.32	1.36	1.36	1.14	1.49
Data collection									
θ limits (°)	$2 < \theta < 26$	$2 < \theta < 23$	$2 < \theta < 26$	$2 < \theta < 25$	$2 < \theta < 26$	$2 < \theta < 25$	$2 < \theta < 23$	$2 < \theta < 25$	$2 < \theta < 26$
hkl limits	$-10, 10; -21, 21; -21, 21$	$-9, 8; -14, 14; -20, 21$	$-8, 8; -10, 10; -14, 14$	$-13, 13; -16, 16; -23, 23$	$-14, 14; -17, 17; -24, 23$	$-8, 8; -19, 19; -14, 14$	$-8, 8; -10, 10; -12, 12$	$-11, 11; -22, 22; -18, 18$	$-8, 7; -15, 14; -22, 22$
No. collected refl.	26164	13551	6859	29900	25557	14096	5681	26317	10692
No. ind. refl. (R_{int})	5010 (0.03)	3154 (0.03)	2537 (0.04)	5543 (0.06)	6526 (0.05)	2592 (0.05)	1934 (0.02)	4836 (0.09)	1488 (0.03)
No. observed refl.[¶]	3587	2181	1211	3615	5212	1731	1797	2603	1403
Refinement									
R[¶',§]	0.049	0.071	0.047	0.082	0.063	0.042	0.067	0.065	0.053
R_w[∥',#']	0.133	0.212	0.120	0.182	0.136	0.112	0.221	0.168	0.127
No. of variables	284	347	232	401	440	206	217	314	127
GOOF	1.02	1.05	0.84	1.15	1.15	1.03	1.17	0.96	1.22
$\Delta\rho_{min}$ (e Å⁻³)	-0.20	-0.47	-0.18	-0.21	-0.28	-0.16	-0.30	-0.14	-0.32
$\Delta\rho_{max}$ (e Å⁻³)	0.16	0.51	0.16	0.20	0.42	0.16	0.47	0.19	0.30

[†] Data collection at $T = 293$ K; [‡] Data collection at $T = 100$ K; [¶] $I > 2\sigma(I)$; [§] $R = \sum(F_o^2 - F_c^2)/\sum F_o^2$; [∥] all data; [#] $R_w = [\sum w(F_o^2 - F_c^2)^2/\sum w(F_o^2)^2]^{1/2}$.

TABLE III   Geometrical parameters for the O—H⋯O hydrogen boding interactions in the crystal structures of compounds **1–9**

| Comp.	Motif	Type of interaction	Atom labels	Symmetry code	D_{O-H} (Å)	$D_{H\cdots O}$ (Å)	$D_{O\cdots O}$ (Å)	∠OHO (°)
1	**L**	COOH⋯⁻OOC	O3—H⋯O1′	$-1/2 + x, 1/2 - y, -1/2 + z$	1.20	1.27	2.463(2)	173
		O_w—H⋯⁻OOC	O30—H⋯O2	x, y, z	0.84	1.99	2.817(2)	171
		O_w—H⋯⁻OOC	O30—H⋯O3′	$-1/2 + x, 1/2 - y, -1/2 + z$	0.84	2.24	2.967(2)	146
2	**C**	[—COO⋯H⋯OOC—]⁻	O7—H⋯O1′	$-x, 1/2 + y, 1/2 - z$	1.22	1.24	2.452(3)	176
	D	COOH⋯⁻OOC	O3—H⋯O2′	$1 + x, y, z$	0.86	1.77	2.592(4)	159
		C—H⋯O=C(OH)	C3—H⋯O4′	$-1 + x, y, z$	0.93	2.75	3.676(4)	176
	D	COOH⋯⁻OOC	O9—H⋯O8′	$1 + x, y, z$	0.85	1.73	2.564(4)	166
		C—H⋯O=C(OH)	C11—H⋯O10′	$-1 + x, y, z$	0.93	2.75	3.671(4)	173
	–	O_w—H⋯[O⋯H⋯O]⁻	O30—H⋯O1	x, y, z	–	–	2.862(9)	–
	–	O_w—H⋯O_2N—R	O30—H⋯O11′	$x, 1/2 - y, 1/2 + z$	–	–	3.031(11)	–
3	**C**	[—COO⋯H⋯OOC—]⁻	O1—H⋯O1′	$1 - x, 1 - y, 1 - z$	1.22	1.22	2.442(2)	180
	D	COOH⋯⁻OOC	O3—H⋯O2′	$x, 1 + y, z$	0.89	1.71	2.586(2)	167
		C—H⋯O=C(OH)	C3—H⋯O4′	$x, -1 + y, z$	0.93	2.71	3.637(3)	174
4	**E′**	COOH⋯⁻OOC	O1—H⋯O7′	$1 - x, 1/2 + y, 1/2 - z$	1.19	1.25	2.447(4)	177
		O—H⋯[—COOH⋯OOC −]⁻	O3—H⋯O2′	$1 - x, -1/2 + y, 1/2 - z$	0.81	1.82	2.631(3)	173
		O—H⋯[—COOH⋯OOC—]⁻	O9—H⋯O8′	$2 - x, 1/2 + y, 1/2 - z$	0.87	1.76	2.623(3)	173
5	**E′**	COOH⋯⁻OOC	O1—H⋯O7′	$1 - x, 1/2 + y, 1/2 - z$	1.11	1.36	2.463(3)	176
		O—H⋯[—COOH⋯OOC—]⁻	O3—H⋯O2′	$2 - x, -1/2 + y, 1/2 - z$	0.89	1.79	2.683(3)	175
		O—H⋯[—COOH⋯OOC—]⁻	O9—H⋯O8′	$1 - x, 1/2 + y, 1/2 - z$	0.86	1.78	2.639(3)	175
6	**C**	COOH⋯⁻OOC	O1—H⋯O3′	$3/2 - x, 1/2 + y, 1/2 - z$	0.97	1.63	2.563(2)	159
	I	COOH⋯O_w	O5—H⋯O30′	$1 - x, 1 - y, 1 - z$	0.92	1.70	2.577(2)	160
		O_w—H⋯⁻OOC	O30—H⋯O4′	$-1/2 + x, 1/2 - y, -1/2 + z$	0.84	1.84	2.679(2)	176
	–	O_w—H⋯⁻OOC	O30—H⋯O3	x, y, z	0.84	1.93	2.764(2)	176
7	**C**	[—COO⋯H⋯OOC—]⁻	O1—H⋯O1′	$1 - x, - y, 2 - z$	1.23	1.23	2.457(3)	180
	G	COOH⋯O=C(OH)	O5—H⋯O4′	$x, -1 + y, z$	0.85	1.77	2.593(4)	163
		COOH⋯O_w	O3—H⋯O30	x, y, z	0.97	1.67	2.581(4)	155
		O_w—H⋯O=C(OH)	O30—H⋯O6′	$x, 1 + y, z$	0.84	2.08	2.907(4)	168
	–	O_w—H⋯[O⋯H⋯O]⁻	O30—H⋯O2′	$x, 1 + y, -1 + z$	0.84	2.03	2.865(4)	176
8	**M**	COOH⋯⁻OOC	O1—H⋯O3′	$-1 + x, y, z$	0.92	1.56	2.462(3)	164
		O_w—H⋯⁻OOC	O30—H⋯O4	x, y, z	0.84	1.82	2.657(3)	175
		O_w—H⋯O=C(OH)	O30—H⋯O2′	$1 + x, y, z$	0.84	1.94	2.784(3)	177
	–	COOH⋯O_w	O5—H⋯O30′	$3/2 - x, 1/2 + y, 1/2 - z$	0.87	1.67	2.539(3)	172
9	**C**	[—COO⋯H⋯OOC—]⁻	O1—H⋯O1′	$-x, 1 - y, - z$	1.22	1.22	2.444(2)	180
	–	O—H⋯O⁻ (intra)	O3—H⋯O2	x, y, z	1.04	1.39	2.435(2)	176
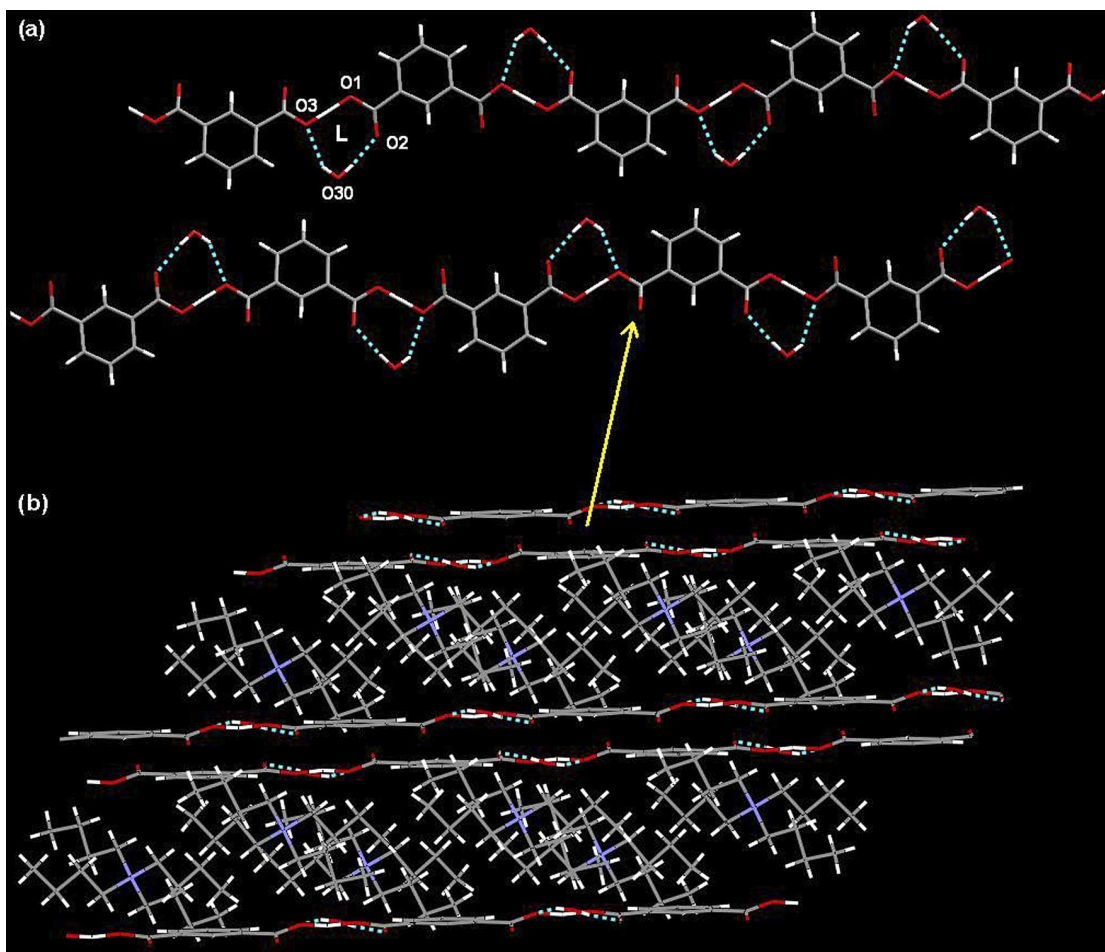
FIGURE 1   (a) Propagation of the hydrogen-bonding motif present in the crystal lattice of [NBu$_4$][HIPA][H$_2$O] (**1**). (b) Supramolecular organization of the anionic tapes and the [NBu$_4$]$^+$ cations.

a significant role in the intermolecular association. The repeating fragments of the hydrogen-bonding motifs found for compounds **2** and **3** are closely related and, therefore, only the case of compound **2** is presented in Fig. 2.

As a comparison with Fig. 1 shows, the carboxyl and carboxylate groups within the [HNIPA][H$_2$-NIPA]$^-$ units are linked now through motifs **C** and **D** (Chart 1). The [RCOO···H···OOCR]$^-$ fragments (motif **C**) have *anti*-configuration and are practically symmetrical (**2**: 1.22 Å, 1.24 Å, 2.452(3) Å, 176°; **3**: 1.22 Å, 1.22 Å, 2.442(2) Å, 180°) with dihedral angles of 178.2° for **2** and 180.0° for **3** [83,84]. They are connected to a linear 1D tape by two additional motifs having a nine-membered cyclic ring (motif **D**) ([RCOOH···OOCR]$^-$: 0.85–0.89 Å, 1.71–1.77 Å, 2.564(4)–2.592(4) Å, 159–167°; C—H···O: 0.93 Å, 2.71–2.75 Å, 3.637(3)–3.676(4) Å, 173–176°). A revision of the CSD gave 588 entries for motif **C** that corresponds to approximately 6% of the carboxylic acid derivatives registered so far [76]. Interestingly, for motif **D** only eight entries have been found, indicating a strong preference for motif **C**. For the eight structures reported so far, the O···O distances for the [RCOOH···OOCR]$^-$ interactions range from

2.511 Å to 2.726 Å, while the C—H···O interactions have values from 3.230 Å to 3.582 Å (Table SI).

The anionic tapes of compounds **2** and **3** contain 24-membered hydrogen-bonded macrocyclic rings with cavities of approximately 2.9 × 4.5 Å^2, and are separated by a perpendicular distance of 3.4 Å within the crystal lattice. Interestingly, these cavities are empty, however, part of the aliphatic groups attached to the ammonium groups are located above and below them (Fig. 2b). Comparing the supramolecular structures of compounds **2** and **3**, it is found that the contents of the asymmetric unit are different, since in the case of **2** water molecules are located among the anionic tapes and the cations. Interestingly, the refinement of the occupancy factor for the water molecules gave a value of only 0.5, and a closer examination of the crystal lattice showed that this is in accordance to the disorder of the NMe$_4^+$ cations. Only for one of the two orientations of the counterions there is enough space for the inclusion of a water molecule, as an examination of the intermolecular O$_w$···NMe$_4^+$ contacts showed. The water molecules participate in two short O$_w$···O (2.863 Å) interactions, one with the [RCOO···H···OOCR]$^-$ fragments and another one with the
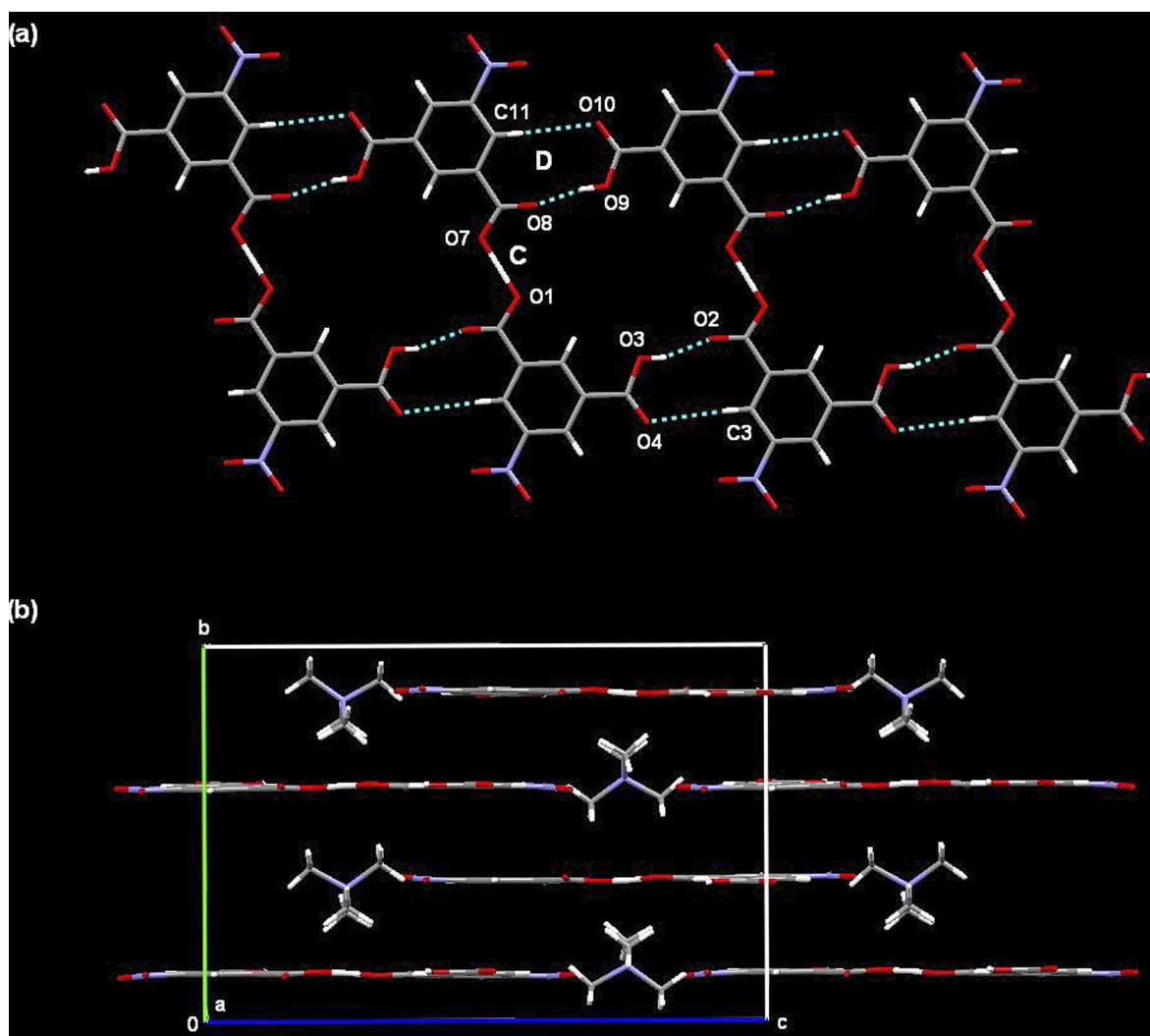
FIGURE 2 (a) Propagation of the hydrogen-bonding motifs present in the crystal lattice of [NMe$_4$][HNIPA][H$_2$NIPA]·0.5[H$_2$O] (**2**). (b) Supramolecular organization between the anionic tapes and the cations in the same compound.

nitro groups (Table III), and C—H···O interactions with the NMe$_4^+$ groups (2.563–2.915 Å, 3.429–3.688 Å, 138–150°).

The crystal lattices of compounds **4** and **5** contain crinkled 2D layers, whose repeating hydrogen-bonding pattern is shown in Fig. 3a for the case of compound **4**. A comparison with Fig. 2a shows that the supramolecular arrangement of the [HNIPA][H$_2$-NIPA]$^-$ moieties has changed significantly. Hydrogen-bonded macrocycles are now formed between three of such fragments, giving a distorted herringbone arrangement. The repeating motif in this assembly contains three hydrogen-bonding interactions, of which the central [RCOO···H···OOCR]$^-$ bond is almost symmetrical (**4**: 1.19 Å, 1.25 Å, 2.447(4) Å, 177°, **5**: 1.11 Å, 1.36 Å, 2.463(3) Å, 176°). The lateral RCOOH···[RCOOH···OOCR]$^-$ bonds are unsymmetrical, but have relatively short O···O distances (0.81–0.89 Å, 1.76–1.82 Å, 2.623(3)–2.683(3) Å, 173–175° for **4** and **5**), thus indicating cooperative assistance [85,86]. This pattern contains

both motifs **C** and **E**′ (Chart 1). So far there is no entry for motif **E**′ in the CSD [76].

The [NR$_4$]$^+$ counterions are localized in the voids left between the crinkled hydrogen-bonded supramolecular layers, the main difference between compounds **4** and **5** being the higher packing density in the latter case ($\delta = 1.32 \leftrightarrow 1.28$ g/cm^3). The similarity between the unit cell parameters should be noticed (Table II). The denser packing of the NBu$_4^+$ salt can be also deduced from the number of C—H···O interactions formed between the anionic layers and the counterions (Table SII).

The comparative analysis of the above discussed ammonium salts **2**–**5** permits to analyze, how the size of the substituents in the tetraalkylammonium cations influences the supramolecular arrangement. While 1D tapes containing tetrameric units are present in the crystal lattices containing the smaller NMe$_4^+$ and NEt$_4^+$ cations, with NPr$_4^+$ and NBu$_4^+$ 2D crinkled layers containing hexameric units are formed. The undulation of the 2D layers and the
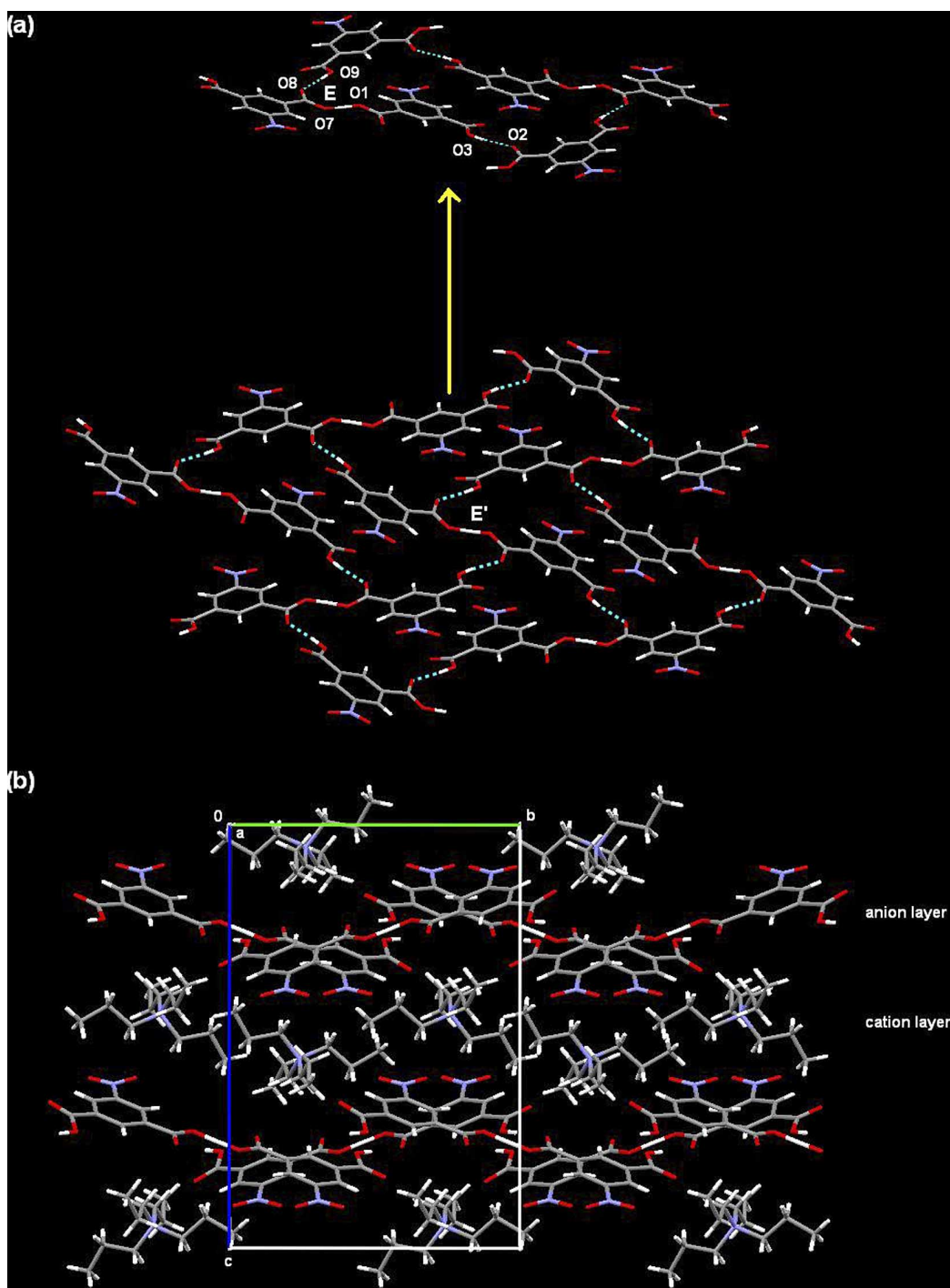
FIGURE 3 (a) Propagation of the hydrogen-bonding motifs present in the crystal lattice of [NPr$_4$][HNIPA][H$_2$NIPA] (**4**). (b) Supramolecular organization between the anionic tapes and the cations in the same compound.

expansion of the tetrameric units to hexameric assemblies can be clearly attributed to the presence of more voluminous cationic counterions. Since only two pairs of different supramolecular structures have been observed for the four salts, it can be also concluded that arrangements with [RCOOH···OOCR]$^-$ hydrogen-bonding interactions possess a certain range of tolerance for empty space within the crystal lattice, before the rearrangement to a more stable packing occurs.

Tetraalkylammonium Dihydrogentrimesates 6–8

Since the structural analyses realized so far have demonstrated that the supramolecular arrangements of molecules containing carboxyl and carboxylate groups can vary depending on the volume of the tetraalkylammonium counterions, we analyzed also the case of trimesic acid (H$_3$TMA), which is momentaneously the most important carboxylic acid in supramolecular chemistry. In this case three

salts gave crystals suitable for X-ray crystallography, compounds **6**–**8** (R = Me, Et and *n*Bu), which all contain water molecules in the crystal lattice (**6**–**8**). For this series the composition of compounds **6** and **8** is identical, [NR$_4$][H$_2$TMA][H$_2$O] with R = Me for **6** and R = *n*Bu for **8**, while compound **7** has a different composition, [NEt$_4$][H$_2$TMA][H$_3$TMA][H$_2$O]$_2$ (**7**). Nevertheless, the hydrogen-bonding patterns are different for all three compounds.

In the crystal lattice of compound **6** a 2D hydrogen-bonded layer is present, which contains 32-membered macrocyclic rings having cavities of 5.2 × 5.6 Å^2 (Fig. 4). Each macrocycle contains two different hydrogen-bonding motifs (**C** in Chart 1 and **I** in Chart 2) that are distributed asymmetrically in the sequence **C-C-I-I**. Interestingly, the [RCOOH···OOCR]$^-$ dimeric unit (0.97 Å, 1.63 Å, 2.563(2) Å, 159°) in motif **C** is asymmetric and has *syn*-configuration with a dihedral angle of only 23.3°, when compared to compounds **1**–**5**, which have *anti*-configuration. In motif **I** the central water molecule links the carboxylate group (0.84 Å, 1.84 Å, 2.679(2) Å, 176°) of the above described motif to the remaining second carboxyl group of the dihydrogentrimesate anion (0.92 Å, 1.70 Å, 2.577(2) Å, 160°), acting simultaneously as hydrogen donor and acceptor.

In the third dimension the anionic layers described above are linked by additional O$_w$—H···$^-$OOCR hydrogen-bonding interactions between the water molecules forming part of one layer and the carboxylate oxygen atoms of the neighboring layer (0.84 Å, 1.93 Å, 2.764(2) Å, 176°). The NMe$_4^+$ cations are located in the cavities formed by the hydrogen-bonded anionic lattice and show eight different C—H···O interactions to the carboxyl and carboxylate groups (0.96 Å, 2.42–2.71 Å, 3.104(3)–3.579(3) Å, 110–166°). Therefore, the cations might have acted as templates during the formation of the supramolecular arrangement. Motif **I** is very uncommon, since a revision of the CSD [76] revealed that it has been found so far only in the crystal structures of thirteen metal carboxylates (Table SIII). There are large variations in the geometric parameters of these motifs, as a consequence of the coordination to metal ions that influences the basicity of the carboxylate groups.

The crystal lattice of compound **7**, [NEt$_4$][H$_2$TMA] [H$_3$TMA][H$_2$O]$_2$, contains crinkled tapes organized along axis *b* that consist of tetrameric units formed by motifs **C** and **G**, which have some similarities with those found in compounds **2** and **3**, but are different from those found for compound **6** (Fig. 5a). The hydrogen-bonded macrocyclic rings have 32 members in this case and cavities of 2.6 × 8.7 Å^2. The geometric parameters found for motif **C** (1.23 Å, 1.23 Å, 2.457(3) Å, 180°) are similar to those determined in the crystal lattices of compounds **2**–**5**. Motif **G** is an extended hydrogen-bonding pattern

of the [RCOOH···HOOCR] dimer due to the incorporation of one water molecule between a donor and an acceptor site (RCOOH···HOOCR: 0.85 Å, 1.77 Å, 2.593(4) Å, 163°). The distances for the O$_w$—H···O = C(OH)R (0.84 Å, 2.08 Å, 2.907(4) Å, 168°) and RCOOH···O$_w$ interactions (0.97 Å, 1.67 Å, 2.581(4) Å, 155°) are significantly larger than those found for motif **I** in compound **6**. Interestingly, there are fourteen further entries in the CSD [76] with the simultaneous presence of both motifs (**C** and **G**) and a comparison of the geometric parameters is given in Table SIV.

Each of the above described tapes is linked to two further tapes through O$_w$—H···$^-$OOCR interactions between the water molecules and the carboxylate groups (0.84 Å, 2.03 Å, 2.865(4) Å, 176°), thus forming the anionic double layers shown in Fig. 5b. The particular shape of the anionic layers allows for the accommodation of the disordered NEt$_4^+$ cations.

Compound **8** has the same composition as compound **6**, however, the hydrogen-bonding pattern is different, thus illustrating the effect the size of the counterions has on the supramolecular structure. The crystal lattice of compound **8** contains crinkled 2D hydrogen-bonded monolayers with trimeric 28-membered macrocycles having cavities of 4.5 × 4.6 Å^2. In the ring formation participate three [H$_2$TMA]$^-$ and three water molecules, which are connected through hydrogen-bonding interactions corresponding to motif **M** (Chart 2, Table III), and additional RCOOH···O$_w$ hydrogen bonds (0.87 Å, 1.67 Å, 2.539(3) Å, 172°) that are formed between uncoordinated carboxyl groups and the water molecules located in the ten-membered cycles mentioned before. Motif **M** can be considered an extension of motif **C**, in which the water molecule acts as twofold donor between the [RCOOH···$^-$OOCR] fragment (0.92 Å, 1.56 Å, 2.462(3) Å, 164°). As expected, the RCOO$^-$···H—O$_w$ interaction (0.84 Å, 1.82 Å, 2.657(3) Å, 175°) is stronger than the RC(OH)O···H—O$_w$ interaction (0.86 Å, 1.94 Å, 2.784(3) Å, 177°). In the CSD there are only three further entries for this motif [76], which have been summarized in Table SV. As shown in Fig. 6b the conformation of the anionic layers is crinkled, most probably as a consequence of the van der Waals and C—H···O interactions with the NBu$_4^+$ cations that are located between them (0.97 Å, 2.39–2.51 Å, 3.366(4)–3.431(4) Å, 152–165°), albeit there are only three C—H···O interactions in this case.

Tetramethylammonium Trihydrogen-pyromellitate 9

The supramolecular assemblies found for the di- and tri-substituted benzenecarboxylic acids described above have shown that the simultaneous presence of carboxyl and carboxylate groups gives a large number of different hydrogen-bonding patterns that
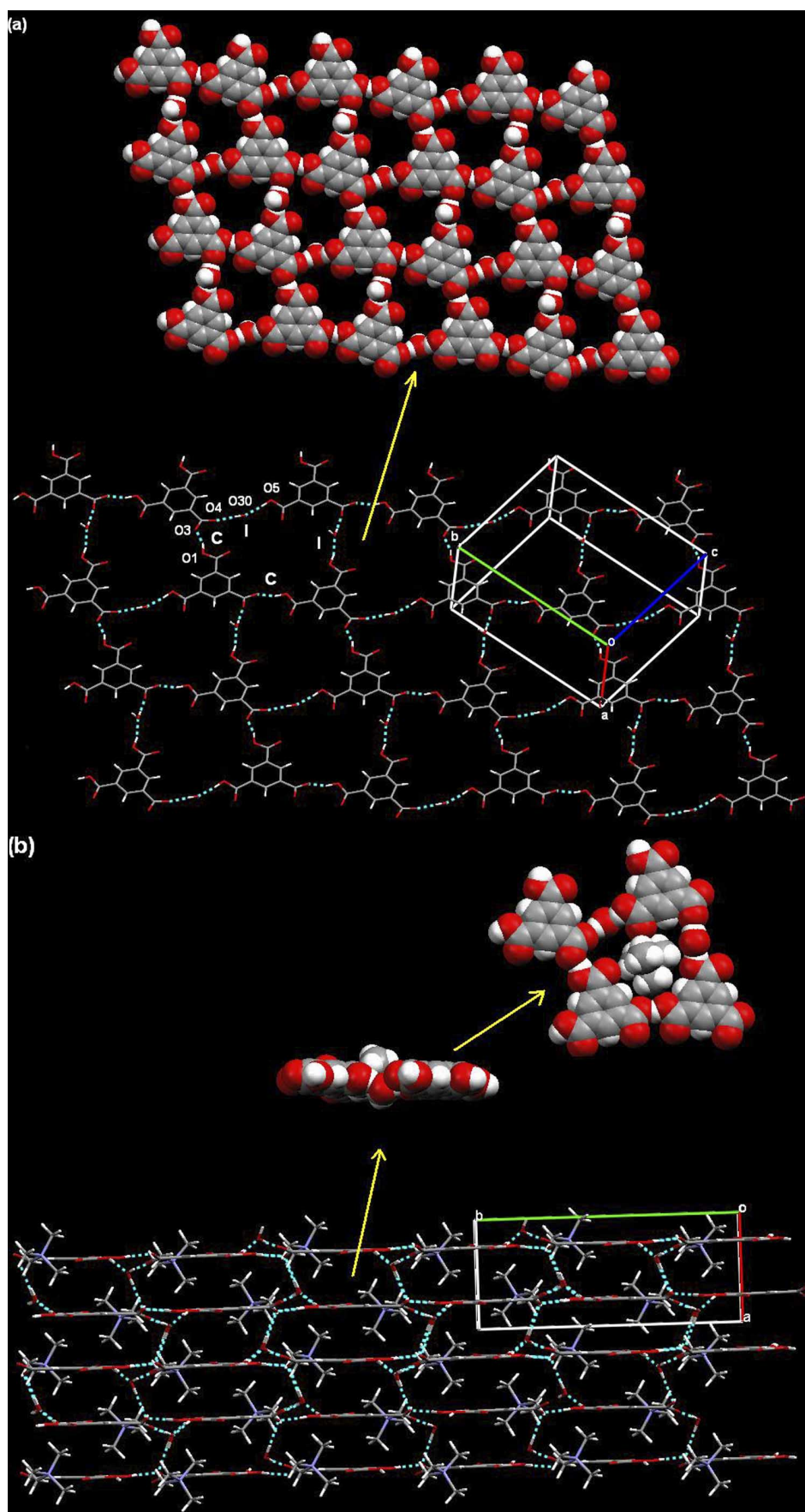
FIGURE 4   (a) Propagation of the hydrogen-bonding motifs present in the crystal lattice of [NMe$_4$][H$_2$TMA][H$_2$O] (**6**). (b) Supramolecular organization between the anionic tapes and the cations.
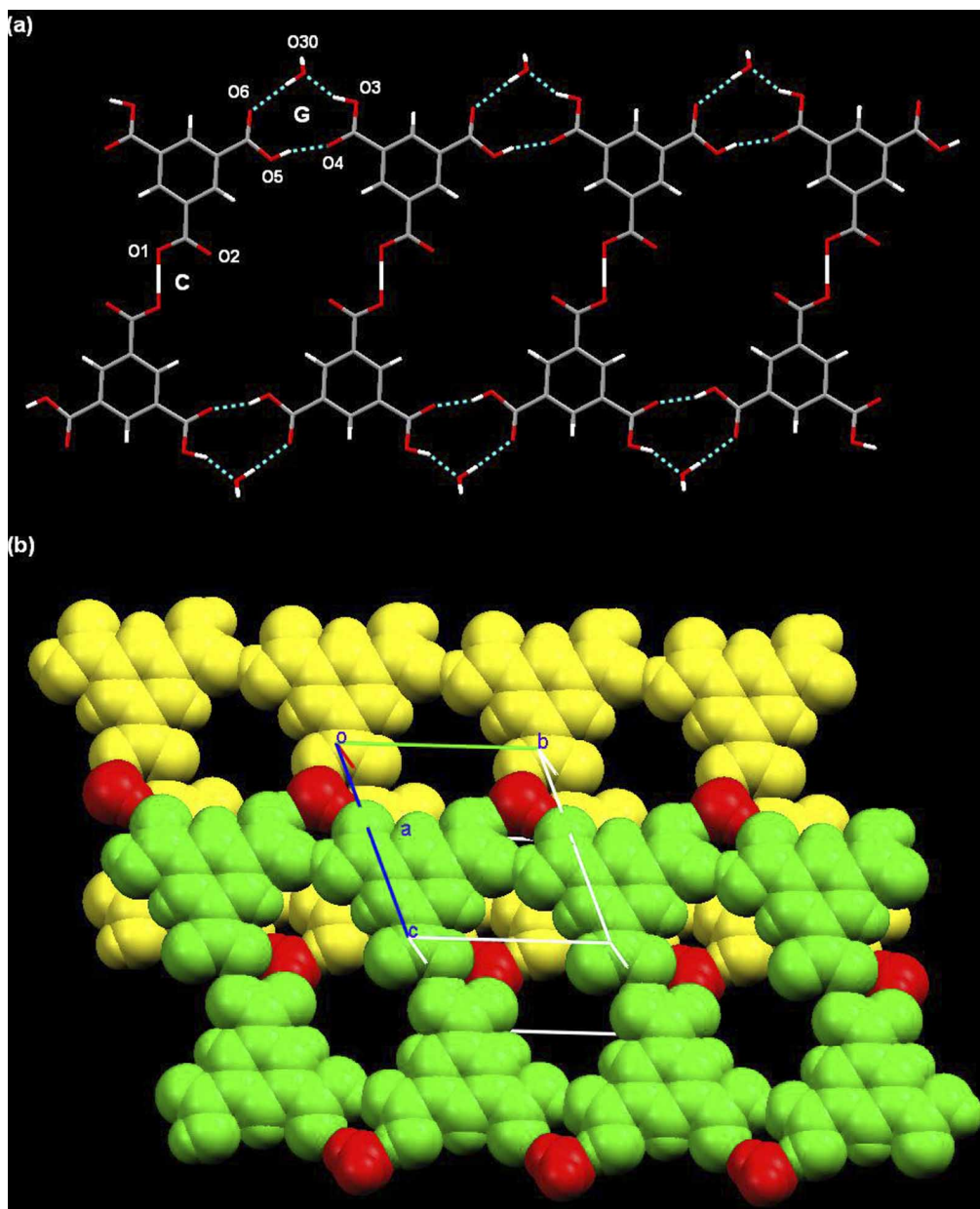
FIGURE 5   (a) Propagation of the hydrogen-bonding motifs present in the crystal lattice of [NEt$_4$][H$_2$TMA][H$_3$TMA][H$_2$O]$_2$ (**7**). (b) Anionic double layers formed through O$_w$—H$\cdots$$^-$OOR interactions.

are influenced by the steric and electronic requirements of guest molecules (e.g., water) or the counterions present in the crystal lattice. In order to collect more information on these systems deprotonation reactions were carried out also between 1,2,4,5-benzenetetracarboxylic acid and the corresponding tetraalkylammonium hydroxides, however, in this case crystals suitable for X-ray diffraction were only obtained for the tetramethylammonium salt **9**, [NMe$_4$][H$_3$PMA].

Due to the proximity of the carboxyl groups in the 1,2 and 4,5 positions of the benzene ring two symmetry-related, intramolecular RCOOH$\cdots$$^-$OOCR/HOOCR hydrogen-bonding interactions are formed for the [H$_3$PMA]$^-$ anion (1.04 Å, 1.39 Å, 2.435(2) Å, 176°), whose geometric parameters are identical due to

the crystallographic mirror symmetry of the molecules. The [H$_3$PMA]$^-$ anions are linked through symmetrical [RCOO$\cdots$H$\cdots$OOCR]$^-$ interactions (1.22 Å, 1.22 Å, 2.444(2) Å, 180°), with a dihedral angle of 180°, thus giving 1D hydrogen-bonded zig–zag chains along axis b (Fig. 7a). Within the crystal lattice the NMe$_4^+$ cations are accommodated in a zig–zag arrangement parallel to the polymeric anionic chains (Fig. 7b), showing a total of ten C—H$\cdots$O interactions (0.98 Å, 2.45–2.65 Å, 3.154(3)–3.552(3) Å, 117–178°).

Theoretical Calculations

In order to obtain more detailed information on the energetic contributions that carboxyl groups can
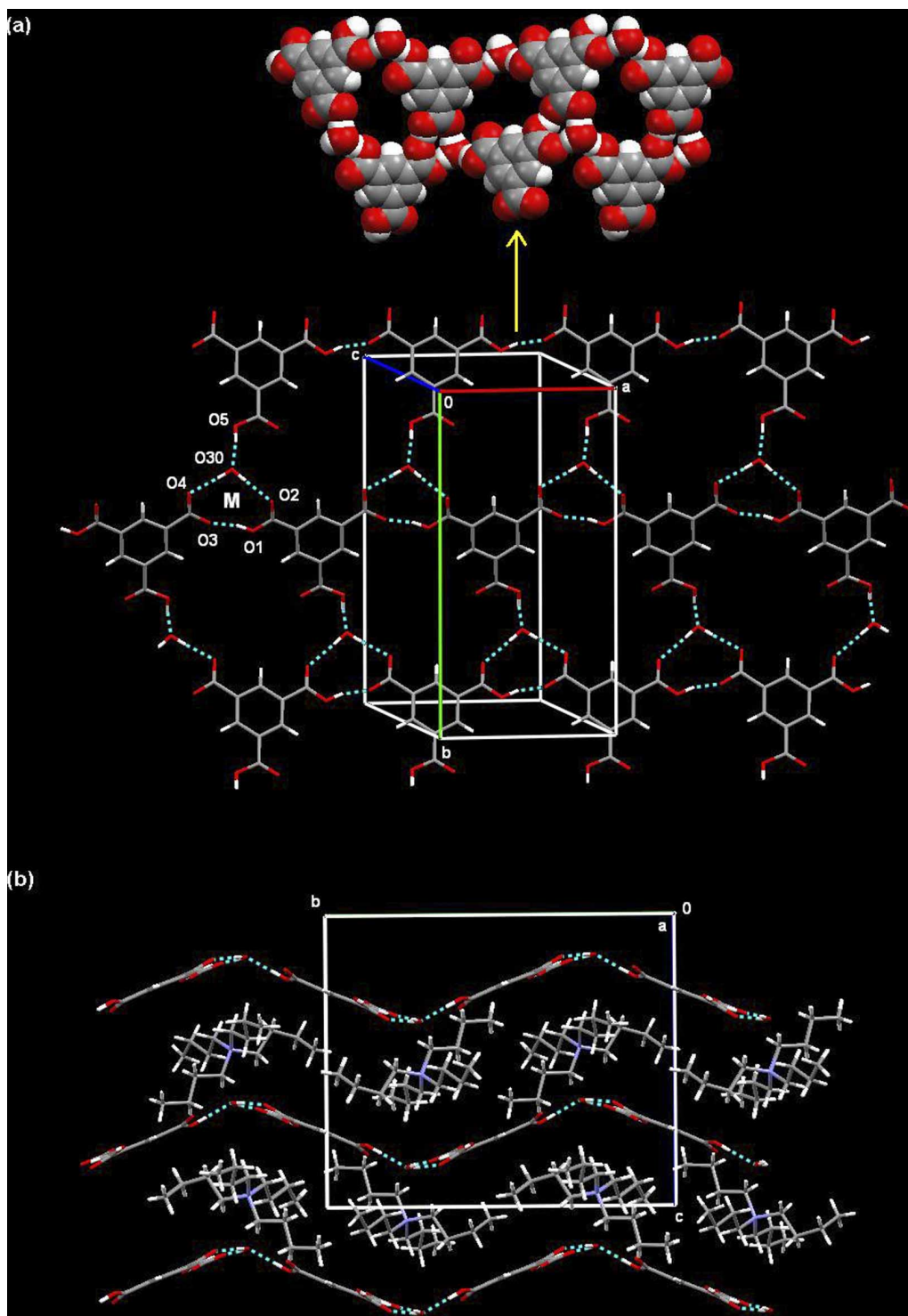
FIGURE 6   (a) Propagation of the hydrogen-bonding motifs present in the crystal lattice of [NBu$_4$][H$_2$TMA][H$_2$O] (**8**). (b) Supramolecular organization between the anionic tapes and the cations.

have in their different hydrogen-bonding patterns to the crystal lattice energy, we determined the hydrogen-bonding geometries and interaction energies for most of the motifs described in Charts 1 and 2 (Fig. 8). Geometry optimizations were performed in the gas phase using ab initio methods at the MP2/6-31G(d,p) level of theory and the *Gaussian98* suite of programs [87,88].

From previous theoretical studies on acetic acid dimers and some other structures containing carboxylic acid moieties it is known that the accurate determination of dimerization energies requires the inclusion of correlation energy as well as the use of large and flexible basis sets, including polarization functions [89–95]. In this work, correlation effects were included at the MP2 level taking into account
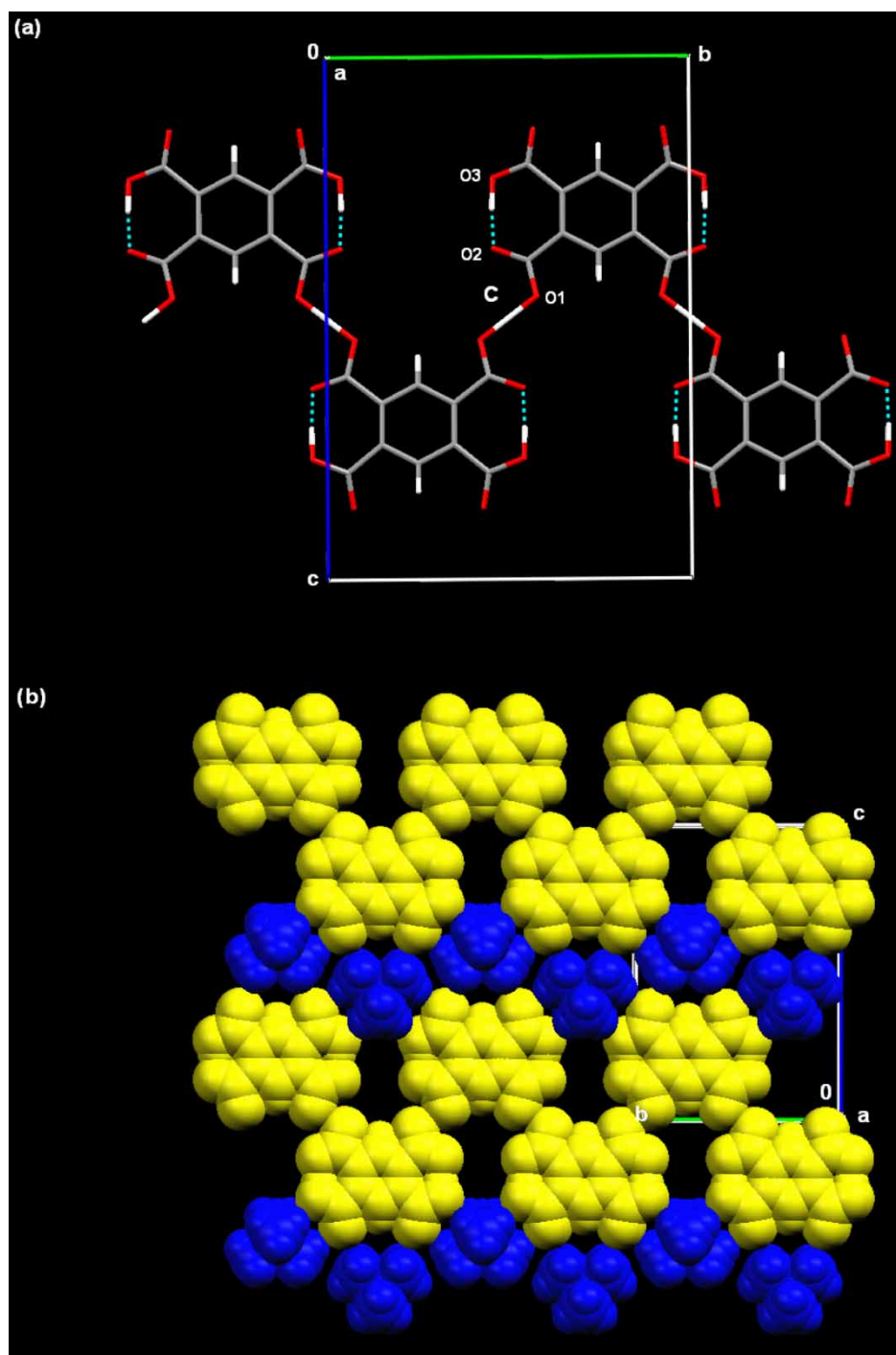
FIGURE 7 (a) Propagation of the hydrogen-bonding motifs present in the crystal lattice of [NMe₄][H₃PMA] (**9**). (b) Supramolecular organization between the anionic tapes and the cations.

the size of the systems and the fact that the interaction energies do not improve significantly when MP4 or QCISD(T) are used instead [90]. Interaction energies were calculated as the difference between the sum of the constituent monomer energies and the energy of the dimer.

For the acetic and benzoic acid dimers the hydrogen-bonding geometries and interaction energies are well established from experimental [96] and theoretical studies [89–92,97–105]. For the

calculations only acetic acid and acetate ions were considered as components in the modeled motifs, since in a previous work it has been reported that the interaction energy difference between the homo-dimeric [RCOOH···HOOCR] motifs containing R = Me and R = Ph is small ($\cong 0.5\,\text{kcal/mol}$) [49]. For neutral motifs the interaction energies were BSSE (basis set superposition error) corrected using a single point counterpoise correction. No attempt was made to correct the charged structures,
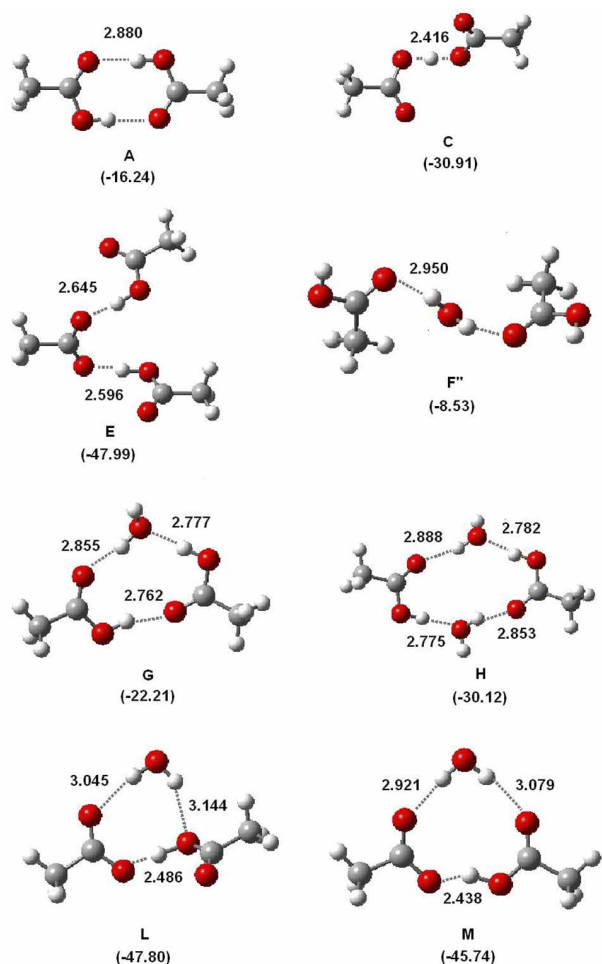
FIGURE 8 Calculated hydrogen-bonding geometries and interaction energies for motifs **A**, **C**, **E**, **F″**, **G**, **H**, **L** and **M**. Note: For the calculation of the motif geometries acetic acid and acetate ions were employed instead of the benzoic acid derivatives found in the crystal structures (*vide supra*).

FIGURE 9   Change of the intermolecular interaction energy of the acetic acid homodimer in dependence of the dihedral angles between the carboxyl groups. The O—H···O distance and bond angle have been frozen.

because it is well-known that ambiguous results can arise [99].

The calculated hydrogen-bonding geometries and interaction energies are given in Figure 8. For motifs **B**, **F**, **F′**, **D** and **I** local minima could not be detected by the geometry optimizations performed in this work (*vide infra*).

Motifs **A** and **B** are the dominant hydrogen-bonding motifs in the crystal structures of neutral carboxylic acids. To understand the factors that favor the transformation of the twofold hydrogen-bonded dimer **A** to the single hydrogen-bonded dimer **B** within a supramolecular structure, we have analyzed the energetic cost required for changing the closed dimer conformation to the open *syn*-conformation, realizing single point calculations at the MP2/6-31G(d,p) level. Figure 9 shows that the increase of the dihedral angle between the carboxyl groups from 0 to 180° destabilizes the system by approximately 11.3 kcal/mol (−16.24 kcal/mol for **A** and −4.96 kcal/mol for *syn*-**B**). This large energy difference has been found also in previous works
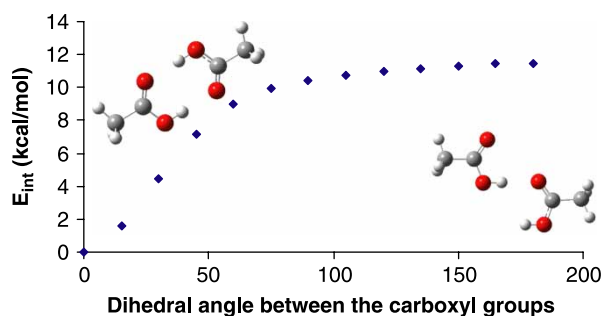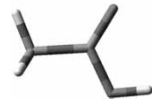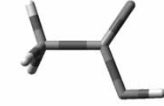
using different levels of calculation [91,92,97]. However, it has to be considered that in the gas phase neither the *syn*- nor the *anti*-conformations of motif **B** correspond to stable structures. During the formation of a crystal lattice the transformation of motif **A** to other conformers or expanded motifs can only be promoted, if further coordination to additional groups capable of hydrogen-bonding promotes the occurrence of extended motifs with more favorable supramolecular interactions.

In motifs **F**, **G**, **H**, **I**, **L** and **M** one or more water molecules are involved. The double acceptor/donor character and the small size provide this molecule with a large orientation and bonding flexibility even in the condensed phase. It can be expected that the stability of the particular motifs is strongly influenced by the hydrogen-bonding pattern of the water molecules. Previously, Gao and Leung have analyzed the hydrogen-bonding geometries and relative stabilities of several acetic acid—monohydrates, using DFT methods and much larger basis sets than those employed herein [102]. To assess the accuracy of the theoretical level used in the present study, we calculated the interaction energies for the three acetic acid—water conformers *syn*-**1**, *syn*-**2** and *syn*-**3**. A comparison with the reported data [102,106] shows that our results are in very good agreement (Table IV).

The difference between motifs **F**, **F′** and **F″** is that the water molecule acts as twofold hydrogen acceptor in the first case, as donor/acceptor in the second case and as twofold donor in the last case. It was not possible to locate a minimum in the potential energy surfaces of motifs **F** and **F′**, which can be explained by the presence of uncoordinated hydrogen atoms at the water molecules (*vide infra*). In contrast, motif **F″** was fully characterized as minimum with an overall interaction energy of −8.53 kcal/mol. There are only very small non-additive contributions for this system (0.30 kcal/mol), which is not surprising since non-additivity is a result of synergic polarization effects that are not present in this structure.

TABLE IV Comparison of the calculated interaction energies (BSSE corrected) for the acetic acid—water conformers *syn*-**1**, *syn*-**2** and *syn*-**3** using different levels of theory (in kcal/mol)

Conformer		DFT/ 6-311++G (3df,3pd)[†]	MP2/6-31G (d,p)[‡]
	syn-**1**[¶]	− 9.55	− 9.54
	syn-**2**	− 5.44	− 4.44
	syn-**3**	− 3.04	− 2.79

[†]Reference [102]; [‡]present study; [¶] − 9.97 kcal/mol using MP2/6-311 + + G** in reference [106].

TABLE V Relative stability of motifs **F″**, **G** and **H** based on the calculated interaction energies (MP2/6-31G(d,p))

Motif	E_{int}[†] (kcal/mol)	ΔE_{int}[‡] (kcal/mol)	$\bar{E}_{int}$[¶] *(kcal/mol)*
F″	− 8.53	–	− 4.26
G	− 22.21	− 15.97	− 7.40
H	− 30.12	− 7.91	− 7.53

[†]Values are BSSE corrected; [‡]$\Delta E_{int} = E_{int}$(motif **G**)—E_{int} (motif **F″**) in the first case and $\Delta E_{int} = E_{int}$(motif **H**)—E_{int} (motif **G**) in the second case; [¶]$\bar{E}_{int}$ = mean interaction energy (per hydrogen-bond).

Motif **G** has the same acid-water ratio as motif **F**, but in this case a cyclic motif with three hydrogen bonds is present, giving a significantly larger interaction energy of $\Delta E_{int} = -22.21$ kcal/mol that is in good agreement with a previous calculation using a larger basis set (−21.41 kcal/mol at the MP2/TZVPP level) [101]. Also in this case, there are only small cooperative effects (1.32 kcal/mol) that account for 5.9% of the overall interaction energy. The hydrogen-bonded ring has a twisted conformation as indicated by the dihedral angles formed between the mean-plane of the system, the carboxyl group (7°) and the water molecule (20°).

Motif **H** involves an additional water molecule and consists of four hydrogen bonds, giving an overall calculated interaction energy of − 30.12 kcal/mol, of which only 1.21 kcal/mol correspond to cooperative effects. This motif has also been studied by Chocholousova *et al.* with DFT methods (B3LYP/6-31G**) that predict a smaller interaction energy (− 23.88 kcal/mol) [101].

A comparative analysis of the interaction energies found for motifs **F″**, **G** and **H** shows that the stability increases in the direction **F″** < **G** < **H**. This can be deduced from the values for the interaction energy differences between the three motifs and the average interaction energies per hydrogen bond shown in Table V. However, in particular the range of the $\bar{E}_{int}$ values reveals that the differences are relatively small ($\Delta \bar{E}_{int} = 3.27$ kcal/mol), explaining that any of these motifs can be found in the condensed phase as a consequence of additional hydrogen-bonding interactions through the uncoordinated hydrogen-bond acceptors and donors.

Motifs containing a carboxylate (**C**, **D**, **E**) have an ion-dipole interaction that is stronger than most dipole–dipole interactions. This is reflected in the interaction energies, as a comparison between the acetic acid dimer and the acetic acid–acetate complex shows [99,103,107–109]. Although the latter contains only one hydrogen bond, the interaction energy is significantly larger (− 16.24 kcal/mol for **A** and − 30.91 kcal/mol for **C**).[49] In order to minimize the repulsion between the oxygen atoms the hydrogen-bonded structure **C** is nonplanar, as indicated by the dihedral angle formed between the four oxygen atoms (− 64.9°). The hydrogen atom is located in the center of the dimeric unit, giving an O···H distance of 1.208 Å. These very short hydrogen bonds are characterized by a very flat potential energy surface that allows the hydrogen atom to move freely between the oxygen atoms [83,84,110]. This sort of delocalization contributes to the stability of the system and its occurrence in the gas-phase has been confirmed for related systems by theoretical calculations and rotavibrational spectroscopy [111]. In the solid state this hydrogen-bonding pattern is frequently asymmetric due to packing effects that provide additional interactions with one or both oxygen atoms. With increasing asymmetry the O···O bond distance should increase as reported by Gilli [86], however, the O···O bond distance can be also influenced significantly by additional interactions [85,86]. Evidence is given by the hydrogen-bonding parameters of compound **8**, that albeit having the most asymmetric RCOOH···⁻OOCR interaction, has a very short O···O distance (0.92 Å, 1.56 Å, 2.462(3) Å, 156° in motif **M**).

The interaction energies for the charged motifs **E**, **L** and **M** are presented in Table VI. All of them have at least two strong charge-assisted hydrogen bonds that give rise to very stable conformations. For motif **D** it was not possible to locate a minimum in the gas phase calculation, probably due to the lack of diffuse functions in the basis set used [95]. Motif **D** appears in two of the crystal lattices described herein (compounds **2** and **3**), and its geometry is strongly influenced by the lattice, since in the gas phase the

TABLE VI   Interaction energies for motifs **C**, **E**, **L**, **M**[†]

Motif	E_{int}[‡] (kcal/mol)	$\bar{E}_{int}$[¶] (kcal/mol)
C	− 30.91	− 30.91
E	− 47.99	− 24.00
L	− 47.80	− 15.93
M	− 45.74	− 15.25

[†] It was not possible to locate a minimum for motifs **D** and **I**, probably due to the lack of diffuse functions in the basis set used; [‡] Values of the charged motifs **C**, **E**, **L** and **M** are **not** BSSE corrected; [¶] $\bar{E}_{int}$ = mean interaction energy (per hydrogen-bond).

C—H···O interaction did not contribute to its stability.

The crystal lattices of compounds **4** and **5** contain motif **E′**. Because of limited calculation time only the simplified motif **E** could be analyzed by theoretical calculations. This motif is non-planar and one of the carboxyl groups is tilt by an angle of 25.6° with respect to the mean plane formed by the carboxylate and the second carboxyl group. In the gas phase calculation the hydrogen bonds are unsymmetrical (H···O: 1.639 Å, 1.809 Å; O···O: 2.450 Å, 2.624 Å), while they are almost symmetrical in the solid state (Table III), as a consequence of the expansion by coordination to an additional RCOOH group (motif **E′**), thus adopting a more symmetrical distribution of the O···O bond lengths (Table III).

Motifs **I**, **L** and **M** are water-expanded motifs of hydrogen-pattern **C**. In the first case the expected donor/acceptor character of the water molecule leaves one uncoordinated hydrogen atom. It was not possible to optimize the geometry of this pattern, since the system re-orientates the water molecule in order to reach a dd/a character, i.e., both hydrogen atoms from the water interact with the carboxylate group and the water oxygen accepts a hydrogen bond from the carboxyl group. This situation and the observation made for motifs **F** and **F′** show that open hydrogen-bonding patterns with dangling protons tend to adopt geometries that are entirely different from those found in the solid state.

In motifs **L** and **M** the water molecules act as twofold donor towards the carboxyl and carboxylate units. A comparison of the hydrogen-bonding geometries shows that the O···O distances are significantly shorter for motif **M** (Fig. 8), however, the interaction energies indicate an increased stability for motif **L** (−47.80 kcal/mol for **L** and −45.74 kcal/mol for **M**). In the solid state the O···O distances follow the same trend as in the gas phase, and again the occurrence of motif **M** can be attributed to the existence of additional hydrogen-bonding interactions. While in compound **1** motif **L** participates only in a C—H···O interaction, motif **M** (in compound **8**) is involved in strong hydrogen-bonding interactions with a carboxylate group in an adjacent layer.

CONCLUSIONS

The results discussed in this contribution have shown that hydrogen-bonding motifs formed between carboxyl and carboxylate groups are more favored than the neutral homodimeric unit typically observed for carboxylic acids, which has not been observed in any of the structures described herein. The reason is that motifs with —[RCOOH···OOCR]⁻ junctions have significantly higher interaction energies, as it has been shown by theoretical calculations. Since the [RCOOH···OOCR]⁻ fragment contains only a single hydrogen bond, it can participate in further hydrogen-bonding interactions, e.g., with water molecules, giving a large number of different hydrogen-bonding patterns. Since their interaction energies are quite similar, it will be difficult to predict the formation of a specific motif a priori, when designing a supramolecular reaction. This is also demonstrated by the fact that the steric volume of tetraalkylammonium ions has an important influence on the configuration and conformation of the supramolecular structure within a crystal lattice, although they are involved only in relatively weak intermolecular interactions, mainly C—H···O and van-der-Waals contacts. This work evidences also that [RCOOH···OOCR]⁻ interactions should be far more important in biochemical environments than [RCOOH···HOOCR] interactions, considering that molecules containing carboxyl and amino groups are zwitterionic in aqueous solution.

References

[1] Aakeröy, C. B.; Seddon, K. R. *Chem. Soc. Rev.* **1993**, 397.
[2] MacDonald, J. C.; Whitesides, G. M. *Chem. Rev.* **1994**, *94*, 2383.
[3] Desiraju, G. R. *Angew. Chem. Int. Ed. Engl.* **1995**, *34*, 2311.
[4] Subramanian, S.; Zawarotko, M. J. *Coord. Chem. Rev.* **1994**, *137*, 357.
[5] Desiraju, G. R. *Chem. Commun.* **1997**, 1475.
[6] Braga, D.; Grepioni, F.; Desiraju, G. R. *Chem. Rev.* **1998**, *98*, 1375.
[7] Krische, M. J.; Lehn, J.-M. *Struct. and Bonding* **2000**, *96*, 3.
[8] Prins, L. J.; Reinhoudt, D. N.; Timmerman, P. *Angew. Chem. Int. Ed.* **2001**, *40*, 2383.
[9] Ermer, O.; Eling, A. *Angew. Chem. Int. Ed. Engl.* **1988**, *27*, 829.
[10] Ermer, O. *J. Am. Chem. Soc.* **1988**, *110*, 3737.
[11] Ermer, O.; Lindenberg, O. *Helv. Chim. Acta*. **1991**, *74*, 825.
[12] Yang, J.; Marendaz, J.-L.; Geib, S.J.; Hamilton, A.D. *Tetrahedron Lett.* **1994**, *35*, 3665.
[13] Kolotochin, S. V.; Fenlon, E. E.; Wilson, S. R.; Loweth, C. J.; Zimmerman, S. C. *Angew. Chem. Int. Ed. Engl.* **1995**, *34*, 2654.
[14] Zimmerman, S. C.; Zeng, F.; Reichert, D. E. C.; Kolotochin, S. V. *Science* **1996**, *271*, 1095.
[15] Zafar, A.; Yang, J.; Geib, S. J.; Hamilton, A. D. *Tetrahedron Lett.* **1996**, *37*, 2327.
[16] Kolotochin, S. V.; Thiessen, P. A.; Fenlon, E. E.; Wilson, S. R.; Loweth, C. J.; Zimmerman, S. C. *Chem. Eur. J.* **1999**, *5*, 2537.

[17] Chatterjee, S.; Pedireddi, V. R.; Ranganathan, A.; Rao, C. N. R. *J. Mol. Struct.* **2000**, *520*, 107.

[18] Holy, P.; Zavada, J.; Zezula, J.; Cisarova, I.; Podlaha, J. *Collect. Czech. Chem. Commun.* **2001**, *66*, 820.

[19] Bhogala, B. R.; Vishweshwar, P.; Nagia, A. *Cryst. Growth Des.* **2002**, *2*, 325.

[20] Shan, N.; Bond, A. D.; Jones, W. *Cryst. Eng.* **2002**, *5*, 9.

[21] Field, J. E.; Combariza, M. Y.; Vachet, R. W.; Venkataraman, D. *Chem. Commun.* **2002**, 2260.

[22] Arora, K. K.; Pedireddi, V. R. *J. Org. Chem.* **2003**, *68*, 9177.

[23] Laliberté, D.; Maris, T.; Wuest, J. D. *Can. J. Chem.* **2004**, *82*, 386.

[24] Bhogala, B. R.; Basavoju, S.; Nagia, A. *Cryst. Growth Des.* **2005**, *5*, 1683.

[25] Burrows, A. D.; Chan, C.-W.; Chowdry, M. M.; McGrady, J.E.; Mingos, D.M. P. *Chem. Soc. Rev.* **1995**, 329.

[26] Munakata, M.; Wu, L. P.; Yamamoto, M.; Kuroda-Sowa, T.; Maekawa, M. *J. Am. Chem. Soc.* **1996**, *118*, 3117.

[27] Aakeröy, C. B.; Beatty, A. M.; Leinen, D. S. *Angew. Chem. Int. Ed.* **1999**, *38*, 1815.

[28] Brammer, L.; Rivas, J. C. M.; Atencio, R.; Fang, S.; Pigge, F. C. *J. Chem. Soc., Dalton Trans.* **2000**, 3855.

[29] Burrows, A. D.; Harrington, R. W.; Mahon, M. F.; Price, C. E. *J. Chem. Soc. Dalton Trans.* **2000**, 3845.

[30] Beatty, A. M. *Cryst. Eng. Commun.* **2001**, *51*, 1.

[31] Burrows, A. D.; Harrington, R. W.; Mahon, M. F.; Teat, S. J. *Cryst. Eng. Commun.* **2002**, 539.

[32] Burke, N. J.; Burrows, A. D.; Donovan, A. S.; Harrington, R. W.; Mahon, M. F.; Price, C.E. *J. Chem. Soc., Dalton Trans.* **2003**, 3840.

[33] Aakeröy, C. B.; Beatty, A. M.; Desper, J.; O'Shea, M.; Valdes-Martínez, J. *J. Chem. Soc., Dalton Trans.* **2003**, 3956.

[34] Beatty, A. M. *Coord. Chem. Rev.* **2003**, *246*, 131.

[35] Kitagawa, S.; Uemura, K. *Chem. Soc. Rev.* **2005**, *34*, 109.

[36] Ding, B.-B.; Weng, Y.-Q.; Mao, Z.-W.; Lam, C.-K.; Chen, X.-M.; Ye, B.-H. *Inorg. Chem.* **2005**, *44*, 8836.

[37] George, S.; Goldberg, I. *Cryst. Growth Des.* **2006**, *6*, 755.

[38] Braga, D.; Grepioni, F.; Desiraju, G. R. *Chem. Rev.* **1998**, *98*, 1375.

[39] Braga, D. *J. Chem. Soc., Dalton Trans.* **2000**, 3705.

[40] Desiraju, G. R. *J. Chem. Soc., Dalton Trans.* **2000**, 3745.

[41] Braga, D.; Maini, L.; Grepioni, F.; Elschenbroich, C.; Paganelli, F.; Schiemann, O. *Organometallics* **2001**, 1875.

[42] Shin, D. M.; Chung, Y. K.; Lee, I. S. *Cryst. Growth Des.* **2002**, *2*, 493.

[43] Braga, D.; Polito, M.; D'Addario, D.; Grepioni, F. *Cryst. Growth Des.* **2004**, *4*, 769.

[44] Leiserowitz, L. *Acta Cryst. B* **1976**, *32*, 775.

[45] Frankenbach, G. M.; Etter, M. C. *Chem. Mater.* **1992**, *4*, 272.

[46] Allen, F. H.; Raithby, P. R.; Shields, G. P.; Taylor, R. *Chem. Commun.* **1998**, 1043.

[47] Allen, F. H.; Motherwell, W. D.S.; Raithby, P. R.; Shields, G. P.; Taylor, R. *New J. Chem.* **1999**, *23*, 25.

[48] Davey, R. J.; Dent, G.; Mughal, R. K.; Parveen, S. *Cryst. Growth. Des.* **2006**, *6*, 1788.

[49] Rodríguez-Cuamatzi, P.; Arillo-Flores, O. I.; Bernal-Uruchurtu, M. I.; Höpfl, H. *Cryst. Growth Des.* **2005**, *5*, 167.

[50] Plaut, D. J.; Lund, K. M.; Ward, M. D. *Chem. Commun.* **2000**, 769.

[51] Mak, T. C. W.; Xue, F. *J. Am. Chem. Soc.* **2000**, *122*, 9860.

[52] MacLean, E. J.; Teat, S. J.; Farrell, D. M. M.; Ferguson, G.; Glidewell, C. *Acta Cryst. C* **2002**, *58*, o470.

[53] Zakaria, C. M.; Ferguson, G.; Lough, A. J.; Glidewell, C. *Acta Cryst.* **2002**, *B58*, 786.

[54] Babb, J. E. V.; Burke, N. J.; Burrows, A. D.; Mahon, M. F.; Slade, D. M. K. *Cryst. Eng. Commun.* **2003**, *5*, 226.

[55] Karle, I.; Gilardi, R. D.; Rao, C. C.; Muraleedharan, K. M.; Ranganathan, S. *J. Chem. Cryst.* **2003**, *33*, 727.

[56] Raj, S. B.; Stanley, N.; Muthiah, P. T.; Bocelli, G.; Olla, R.; Cantoni, A. *Cryst. Growth Des.* **2003**, *3*, 567.

[57] Trivedi, D. R.; Ballabh, A.; Dastidar, P. *Cryst. Eng. Commun.* **2003**, *5*, 358.

[58] Yang, C.; Wong, W.-T. *Chem. Lett.* **2004**, *33*, 856.

[59] Kobayashi, N.; Naito, T.; Inabe, T. *Cryst. Eng. Commun.* **2004**, *6*, 189.

[60] Lam, C.-K.; Xue, F.; Zhang, J.-P.; Chen, X.-M.; Mak, T. C. W. *J. Am. Chem. Soc.* **2005**, *127*, 11536.

[61] Gobetto, R.; Nervi, C.; Chierotti, M. R.; Braga, D.; Maini, L.; Grepioni, F.; Harris, R. K.; Hodgkinson, P. *Chem. Eur. J.* **2005**, *11*, 7461.

[62] Sada, K.; Tani, T.; Shinkai, S. *Synlett* **2006**, 2364.

[63] Trivedi, D. R.; Dastidar, P. *Cryst. Growth Des.* **2006**, *6*, 2114.

[64] Said, F. F.; Ong, T.-G.; Bazinet, P.; Yap, G. P. A.; Richeson, D. S. *Cryst. Growth Des.* **2006**, *6*, 1848.

[65] Perrin, C. L.; Nielson, J. B. *Ann. Rev. Phys. Chem.* **1997**, *48*, 511.

[66] Jeffrey, G. A. *An Introduction to Hydrogen Bonding*; Oxford University Press: New York, 1997; p 33.

[67] Meot-Ner, M. *Chem. Rev.* **2005**, *105*, 213.

[68] Mazik, M.; Cavga, H. *J. Org. Chem.* **2006**, *71*, 2957.

[69] Bruker Analytical X-ray Systems. SMART: Bruker Molecular Analysis Research Tool, Version 5.618, **2000**.

[70] Bruker Analytical X-ray Systems. SAINT + NT, Version 6.04, **2001**.

[71] Sheldrick, G. M. *SHELX86, Program for Crystal Structure Solution*; University of Göttingen: Göttingen, Germany, **1986**.

[72] Bruker Analytical X ray Systems. SHELXTL-NT, Version 6.10, **2000**.

[73] Bruno, I. J.; Cole, J. C.; Edgington, P. R.; Kessler, M.; Macrae, C. F.; McCabe, P.; Pearson, J.; Taylor, R. *Acta Cryst.* **2002**, *B58*, 389 (Mercury, *New Software for searching the Cambridge Structural Database and visualizing crystal structures*, version 1.4.1).

[74] PLATON, version 210103, Spek, A.L. *Acta Cryst.* **1990**, *A46*, C-34.

[75] WinGX, Version v1.64.05., 2003, Farrugia, L.J. *J. Appl. Cryst.* **1999**, *32*, 837.

[76] Allen, F. H. *Acta Cryst.* **2002**, *B58*, 380 (The Cambridge Structural Database: A quarter of a million crystal structures and rising, Cambridge Crystallographic Data Centre, version 5.25, November 2003, Cambridge, UK).

[77] Taylor, R.; Kennard, O. *J. Am. Chem. Soc.* **1982**, *104*, 5063.

[78] Desiraju, G. R. *Acc. Chem. Res.* **1991**, *24*, 290.

[79] Steiner, T. *Chem. Commun.* **1997**, 727.

[80] Nangia, A.; Desiraju, G. R. *Acta Cryst.* **1998**, *A54*, 934.

[81] Steiner, T. *New J. Chem.* **1998**, *22*, 1099.

[82] Desiraju, G. R. *Acc. Chem. Res.* **2002**, *35*, 565.

[83] Barry, J. E.; Finkelstein, M.; Ross, S. D.; Mateescu, G. D.; Valeriu, A. *J. Org. Chem.* **1988**, *53*, 6058.

[84] Perrin, C. L.; Thoburn, J. D. *J. Am. Chem. Soc.* **1992**, *114*, 8559.

[85] Vishweshwar, P.; Nangia, A.; Lynch, V. M. *Chem. Commun.* **2001**, 179.

[86] Gilli, G.; Gilli, P. *J. Mol. Struct.* **2000**, *552*, 1.

[87] Hehre, R. D. W. J.; Pople, J. A. *J. Chem. Phys.* **1972**, *56*, 2257.

[88] Frisch, M. J.; Trucks, G. W.; Schlegel, H. B.; Scuseria, G. E.; Robb, M. A.; Cheeseman, J. R.; Zakrzewski, V. G.; Montgomery, J. A., Jr.; Stratmann, R. E.; Burant, J. C.; Dapprich, S.; Millam, J. M.; Daniels, A. D.; Kudin, K. N.; Strain, M. C.; Farkas, O.; Tomasi, J.; Barone, V.; Cossi, M.; Cammi, R.; Mennucci, B.; Pomelli, C.; Adamo, C.; Clifford, S.; Ochterski, J.; Petersson, G. A.; Ayala, P.Y.; Cui, Q.; Morokuma, K.; Rega, N.; Salvador, P.; Dannenberg, J. J.; Malick, D. K.; Rabuck, A. D.; Raghavachari, K.; Foresman, J. B.; Cioslowski, J.; Ortiz, J. V.; Baboul, A. G.; Stefanov, B. B.; Liu, G.; Liashenko, A.; Piskorz, P.; Komaromi, I.; Gomperts, R.; Martin, R. L.; Fox, D. J.; Keith, T.; Al-Laham, M. A.; Peng, C. Y.; Nanayakkara, A.; Challacombe, M.; Gill, P. M. W.; Johnson, B.; Chen, W.; Wong, M. W.; Andres, J. L.; Gonzalez, C.; Head-Gordon, M.; Replogle, E. S.; Pople, J. A. *Gaussian 98*; Revision A.11.3; Gaussian, Inc.: Pittsburgh, PA, 2002.

[89] Meot-Ner (Mautner), M.; Elmore, D. E.; Scheiner, S. *J. Am. Chem. Soc.* **1999**, *121*, 7625.

[90] Colominas, C.; Teixido, J.; Cemelí, J.; Luque, F. J.; Orozco, M. *J. Phys. Chem. B* **1998**, *102*, 2269.

[91] Nakabayashi, T.; Sato, H.; Hirata, F.; Nishi, N. *J. Phys. Chem. A* **2001**, *105*, 245.

[92] Nakabayashi, T.; Nishi, N. *J. Phys. Chem. A* **2002**, *106*, 3491.

[93] Gora, R. W.; Grabowski, S. J.; Leszczynski, J. *J. Phys. Chem. A* **2005**, *109*, 6397.

[94] Van Duijneveldt-van de Rijdt, J. G. C. M.; Van Duijneveldt, F. B. In *Theoretical Treatments of Hydrogen Bonding*; Hadzi, D., Ed.; John Wiley & Sons: Chichester, UK, 1997; pp 13–48.

[95] Novoa, J. J.; Mota, F.; D'Oria, E. In *Hydrogen Bonding—New Insights, Series: Challenges and Advances in Computational*

Chemistry and Physics; Grabowski, S. J., Ed.; Springer: Dordrecht, The Netherlands, 2006; Vol. 3.

[96] Derissen, J. L. *J. Mol. Struct.* **1971**, *7*, 67.

[97] Turi, L.; Dannenberg, J. J. *J. Phys. Chem.* **1993**, *97*, 12197.

[98] Turi, L.; Dannenberg, J. J. *J. Am. Chem. Soc.* **1994**, *116*, 8714.

[99] Dannenberg, J. J.; Paraskevas, L. R.; Sharma, V. *J. Phys. Chem. A* **2000**, *104*, 6617.

[100] Chang, H.-C.; Jiang, J.-C.; Lin, M.-S.; Kao, H.-E.; Feng, C.-M.; Huang, Y.-C.; Lin, S. H. *J. Chem. Phys.* **2002**, *117*, 3799.

[101] Chocholouslova, J.; Vacek, J.; Hobza, P. *J. Phys. Chem. A* **2003**, *107*, 3086.

[102] Gao, Q.; Leung, K. T. *J. Chem. Phys.* **2005**, *123*, 074325.

[103] Aquino, A. J. A.; Tunega, D.; Haberhauer, G.; Gerzabek, M. H.; Lischka, H. *J. Phys. Chem. A* **2002**, *106*, 1862.

[104] Burneau, A.; Génin, F.; Quilès, F. *Phys. Chem. Chem. Phys.* **2000**, *2*, 5020.

[105] Palafox, M. A.; Núñez, J. L.; Gil, M. *Int. J. Quantum Chem.* **2002**, *89*, 1.

[106] Nagy, P. I.; Smith, D. A.; Alagona, G.; Ghio, C. *J. Phys. Chem.* **1994**, *98*, 486.

[107] Kumar, G. A.; McAllister, M. A. *J. Am. Chem. Soc.* **1998**, *120*, 3159.

[108] McAllister, M. A. *Can. J. Chem.* **1997**, *75*, 1195.

[109] Pan, Y.; McAllister, M. A. *J. Mol. Struct.: Theochem.* **1998**, *427*, 221.

[110] Bernal-Uruchurtu, M. I.; Ruiz-López, M. F. *Chem. Phys. Lett.* **2000**, *330*, 118.

[111] Jiang, J.-C.; Wang, Y.-S.; Chang, H.-C.; Lin, S. H.; Lee, Y. T.; Niedner-Schatteburg, G.; Chang, H.-C. *J. Am. Chem. Soc.* **2000**, *122*, 1398.